



Identification and functional clustering of global gene expression differences between human age-related cataract and clear lenses

John R. Hawse,^{1,2} James F. Hejtmancik,³ Qingling Huang,⁴ Nancy L. Sheets,² Douglas A. Hosack,⁵ Richard A. Lempicki,⁵ Joseph Horwitz,⁴ Marc Kantorow¹

¹Biomedical Sciences, Florida Atlantic University, Boca Raton, FL; ²Department of Biology, West Virginia University, Morgantown, WV; ³OGVFB/NIH, Bethesda, MD; ⁴UCLA School of Medicine, Jules Stein Eye Institute, Los Angeles, CA; ⁵Laboratory of Immunopathogenesis and Bioinformatics, SAIC Frederick Inc., Frederick, MD

Purpose: Age-related cataract is a multi-factorial disease with a poorly understood etiology. Numerous studies provide evidence that the human eye lens has evolved specific regulatory and protective systems to ameliorate lens damage associated with cataract. Other studies suggest that the presence of cataract is associated with the altered expression of specific genes including metallothionein IIa, osteonectin, transglutaminase 2, betaig-h3, multiple ribosomal proteins, ADAM9, and protein phosphatase 2A. Here, we sought to identify further gene expression changes that are associated with cataract and to cluster the identified genes into specific biological pathways.

Methods: Oligonucleotide microarray hybridization was used to analyze the full complement of gene expression differences between lens epithelia isolated from human age-related cataract relative to clear lenses. The expression levels of a subset of the identified genes were further evaluated by semi-quantitative RT-PCR. The identified genes were functionally clustered into specific categories and the probability of over-representation of each category was determined using the computer program EASE.

Results: 412 transcripts were observed to be increased and 919 transcripts were observed to be decreased by 2 fold or more in lens epithelia isolated from age-related cataract relative to clear lenses. Of these, 74 were increased and 241 were decreased at the 5 fold level or greater. Seventeen genes selected for further confirmation exhibited similar trends in expression when examined by RT-PCR using both the original and separately prepared clear and cataract RNA populations. Functional clustering of the identified genes using the EASE bioinformatics software package revealed that, among others, transcripts increased in cataract are associated with transcriptional control, chromosomal organization, ionic and cytoplasmic transport, and extracellular matrix components while transcripts decreased in cataract are associated with protein synthesis, defense against oxidative stress, heat-shock/chaperone activity, structural components of the lens, and cell cycle control.

Conclusions: These data suggest that cataract is associated with multiple previously identified and novel changes in lens epithelial gene expression and they point to numerous pathways likely to play important roles in lens protection, maintenance, and age-related cataract.

The role of the eye lens is to focus incoming light onto the retina where visual information is then processed and transmitted to the brain. The lens is an excellent model for the study of age related diseases since it has no blood supply, contains some of the oldest cells in the body, grows throughout life, and is exposed to multiple environmental insults including toxic metals and UV-light which can result in oxidative stress [1]. Oxidative stress, combined with aging of the lens and consequential lens cell damage, is believed to contribute to age-related cataract formation, an opacity of the lens that results in blindness [1]. Cataract is a major health issue worldwide as it is the leading cause of world blindness. Surgical removal of the lens is the only known treatment. Cataract is an enormous economic burden, accounting for 12% of all Medicare expenses in the United States each year. With an

aging American population cataract is, and will continue to be, a major economic and quality of life concern.

Despite the large number of studies documenting the biochemical and metabolic changes in the lens associated with age-related cataract, little is known about the changes in gene expression associated with this disease. To identify these changes we have focused on the lens epithelium since this monolayer of cells is essential for the growth, differentiation, and homeostasis of the entire organ [2,3]. The lens epithelium contains the highest levels of enzymes and transport systems in the lens [4-6] and is the first part of the lens exposed to environmental insults [5,6]. Multiple studies suggest that the lens epithelium is capable of communicating with the underlying fiber cells [7] and direct damage to the lens epithelium and its enzyme systems is known to result in cataract formation [1,8-10]. Importantly, the majority of transcription occurs in the epithelial cells of the lens, and therefore these cells make up the majority of lens cells capable of responding to environmental insults and/or the presence of cataract through

Correspondence to: Marc Kantorow, Ph.D., Florida Atlantic University, Biomedical Sciences, 777 Glades Road, PO Box 3091, Boca Raton, FL, 33431-0991; Phone: (561) 297-2910; email: mkantorow@fau.edu

altered gene expression. Since the lens epithelium is composed of a single cell-type it represents an ideal model for gene expression studies.

Although a multitude of lens culture studies have documented changes in the expression of numerous genes in response to H₂O₂, toxic metals, UV-light, and other stresses, and multiple studies have examined changes in gene expression in animal models of cataract, the full complement of gene expression differences that occur in lens epithelial cells of human age-related cataract is not known. Previous studies have used RT-PCR differential display and other techniques to identify differences in gene expression between human lens epithelial cells isolated from cataract relative to clear lenses. For instance, metallothionein IIa [11], osteonectin (also known as SPARC [12]), transglutaminase 2 [13], and betaig-h3 [14], are reported to be increased in cataract relative to clear lenses while multiple ribosomal proteins [15], ADAM9 [16], and protein phosphatase 2A [11] are reported to be decreased in cataract relative to clear lenses.

While these studies have provided important insight into the roles of specific gene expression changes in age-related cataract, information concerning individual gene expression changes is not adequate to reveal related clusters of genes whose identities are necessary to elucidate the biological pathways that are altered in age-related cataract. Although recent studies have examined the global changes in gene expression that occur in cultured human lens epithelial cells exposed to H₂O₂, a stress associated with cataract [17,18], to date no comprehensive study has documented the global gene expression changes occurring between human age-related cataract and clear lenses or reported the functional clustering of age-related cataract-specific genes. This information is necessary to identify those biological pathways altered in age-related cataract and is essential towards understanding the molecular basis for this disease. Despite the difficulty in obtaining sufficient numbers of human cataracts and clear lenses for this type of large-scale analysis, it is important that these studies be conducted with actual human lens epithelia since no tissue culture or animal model system can mimic the unique life history, physiology and genetic responses of the human lens.

We have used oligonucleotide microarrays to compare the global gene expression profiles between pooled age-matched human lens epithelia isolated from cataract and clear lenses. We demonstrate that more than 1,300 of the 22,215 genes surveyed have expression levels that differ by 2 fold or more in cataracts compared to clear lenses. Of these, 74 genes are increased and 241 genes are decreased in cataract relative to clear lenses at the level of 5 fold or greater. Functional clustering and over-representation analysis of the identified genes revealed that multiple biological pathways are significantly altered upon cataract formation including chaperones, oxidative stress, protein synthesis, and ion transport pathways. These data provide the basis for designing functional experiments to examine the roles of the identified genes in lens maintenance and protection and they provide insight into those mechanisms that may be important for the development of, and defense against, age-related cataract.

METHODS

Tissue collection and RNA preparation: Central lens epithelial tags (2-3 mm²) were obtained from patients undergoing cataract surgery at the Jules Stein Eye Institute, UCLA School of Medicine. The cataracts are representative of the entire population of patients undergoing cataract surgery and were obtained and classified by the same surgeon, according to a modified version of the Lens Opacities Classification Scale (LOCS)-III grading system. The cataracts used in this study were approximately 70% mixed, 20% nuclear, 5% cortical, and 2% posterior subcapsular. With the exception of cataract-type, age and sex, no further identifying information was available for individual lenses. Clear whole human lenses were obtained from organ donors within 24 h post-mortem by the Lions Eye Bank of Oregon and the West Virginia Eye Bank. Whole lenses were microscopically examined for opacities and those lenses exhibiting opacity were discarded from the present study. Clear lenses were micro-dissected for central epithelium (6-8 mm²) and contaminating fiber cells were removed. A total of 106 cataracts (average age 71.2 years) and 10 clear lens epithelia (average age 64.2 years) were used to obtain a sufficient amounts of RNA (2-5 µg) for the microarray study. An additional 50 cataracts (average age 70.8 years) and 10 clear lens epithelia (average age 63.3 years) were used for the secondary semi-quantitative RT-PCR confirmation studies. Another 50 cataracts (average age 68.7 years) and 10 clear lens epithelia (average age 57.0 years) were used for the control and tertiary semi-quantitative RT-PCR confirmation studies. Total RNA was isolated from these samples using the Trizol method.

Microarray procedure and analysis: The quality and quantity of RNA obtained from the cataract and clear lens epithelial tags was determined using a Bioanalyzer 2100 (Agilent Technologies, Palo Alto, CA) according to the manufacturers protocol. Briefly, a small amount of RNA from each sample was loaded on a microgel, electrophoresed, scanned and analyzed for the quantity and integrity of the 18s and 28s ribosomal RNA bands to ensure that the same amount of RNA was examined for both the cataract and clear lens samples.

First and second strand cDNAs were synthesized from 2-5 µg of total RNA using the SuperScript Double-Stranded cDNA Synthesis Kit (Invitrogen, Gaithersburg, MD) and the oligo-dT₂₄-T7 primer (5'-GGC CAG TGA ATT GTA ATA CGA CTC ACT AT-AGG GAG GCG G-3') according to the manufacturer's instructions. cRNA was synthesized and labeled with biotinylated UTP and CTP by in vitro transcription using the T7 promoter coupled double-stranded cDNA as a template and the T7 RNA Transcript Labeling Kit (ENZO Diagnostics Inc., Farmingdale, NY). Briefly, double-stranded cDNAs synthesized from the previous steps were washed twice with 70% ethanol and resuspended in 22 µl of RNase-free H₂O. The cDNA was incubated with 4 µl each of 10X Reaction Buffer, Biotin Labeled Ribonucleotides, DTT, RNase Inhibitor Mix, and 2 µl of 20X T7 RNA Polymerase for 5 h at 37 °C. The labeled cRNA was separated from unincorporated ribonucleotides by passing through a CHROMA SPIN-100 col-

um (Clontech, Palo Alto, CA) and precipitated at -20 °C for 1 h to overnight.

The cRNA pellet was resuspended in 10 µl of RNase-free H₂O and 10 µg was fragmented by heat and ion-mediated hydrolysis at 95 °C for 35 min in 200 µM Tris-acetate, pH 8.1, 500 mM KOAc, and 150 mM MgOAc. The fragmented cRNA was hybridized for 16 h at 45 °C to HG_U133A oligonucleotide arrays (Affymetrix, Santa Clara, CA) containing 22,283 probe sets representing 22,215 gene or extended sequence tag (EST) sequences. Arrays were washed at 25 °C with 6X SSPE (0.9 M NaCl, 60 mM NaH₂PO₄, 6 mM EDTA, and 0.01% Tween-20) followed by a stringent wash at 50 °C with 100

mM MES, 0.1 M (Na⁺), and 0.01% Tween-20. The arrays were then stained with phycoerythrin-conjugated streptavidin (Molecular Probes, Eugene, OR) and the fluorescence intensities were determined using a laser confocal scanner (Hewlett-Packard, Palo Alto, CA).

The scanned images were analyzed using Microarray Suite 5.0 software (Affymetrix), following user guidelines. Briefly, background signal intensities were calculated and used to determine if the signal intensity of an individual gene was statistically greater than the background intensity value. The signal intensity for each gene was calculated as the average intensity difference, represented by $[\Sigma(\text{PM-MM})/(\text{number of probe})]$

TABLE 1. PRIMERS USED FOR RT-PCR

Gene	Abbreviation	Primer sequence	Annealing temperature	Product length	Cycle number	Accession number
Hsp27-1	Hsp27-1	CGCGCTCAGCCGGCAACTCAG	64	419	27	XM_055937
Hsp27-1	Hsp27-1	AGGGGTGGGCATCCAGGCTAAGG	64	419	27	XM_055937
Hsp27-2	Hsp27-2	TCCTGACCCCCACACTCTACCA	61	421	27	NM_001541
Hsp27-2	Hsp27-2	GCTGCCTCCTCCTTTCCTCTG	61	421	27	NM_001541
aA-crystallin	aA	CCACCTCGGCTCCCTCGTCCTAAG	64	492	25	NM_000394
aA-crystallin	aA	CCATGTCCCAAGAGCGGCACTAC	64	492	25	NM_000394
RPL13a	RPL13a	GTATGCTGCCCCACAAAACCA	58	387	25	XM_027885
RPL13a	RPL13a	CAACGCATGAGGAATTAACAGTCTT	58	387	25	XM_027885
Metallothionein IF	MTIF	GCTTCTCTCTTGAAAGTCC	55	226	30	M10943
Metallothionein IF	MTIF	GGCATCAGTCGACGAGCTG	55	226	30	M10943
Metallothionein IH	MTIH	GAATCCAGTCTCACCTCGG	55	213	30	X64834
Metallothionein IH	MTIH	GACATCAGGCACGACGCTG	55	213	30	X64834
Metallothionein IG	MTIG	GCCTCTTCCCTTCTCGCTTG	55	234	30	XM_048213
Metallothionein IG	MTIG	GACATCAGGCGCAGCAGCTG	55	234	30	XM_048213
Glutathione Peroxidase 1	GPX-1	GACCACCCCAAGCTCATCACC	60	333	30	M21304
Glutathione Peroxidase 1	GPX-1	ATCAACAGGACCAGCACCCATCTC	60	333	30	M21304
Na ⁺ /H ⁺ Exchanger II	Na ⁺ /H ⁺ Ex	GCCATCTGTTTTGCGTTAGTGTTT	56	530	23	AF073299
Na ⁺ /H ⁺ Exchanger II	Na ⁺ /H ⁺ Ex	GTTCGCTGACGGATTTGATAGAGA	56	530	23	AF073299
Serine/ Threonine Protein Kinase	S/T PK	TGTTGGTGGGATTTGCTTACTCT	57	449	23	NM_003607
Serine/ Threonine Protein Kinase	S/T PK	CTTGGGCTGGAACTGAAACCTCT	57	449	23	NM_003607
Na ⁺ /K ⁺ ATPase	Na ⁺ /K ⁺ ATPase	AAAGTACAAAGATTCAGCCAGAG	52	419	23	BC000006
Na ⁺ /K ⁺ ATPase	Na ⁺ /K ⁺ ATPase	GGAGTTTGCCATAGTACGGATAAT	52	419	23	BC000006
Secreted Apoptosis Related Protein	SARP	TTGTAATCCAGTCGGCTTGTCTT	56	478	23	AF017987
Secreted Apoptosis Related Protein	SARP	CTGGCCTTTGCTGTCACTATTAC	56	478	23	AF017987
Pleiotrophin	Ple.	GTTCCCCGCTTCCAGTCCA	60	430	23	M57399
Pleiotrophin	Ple.	TGCCAGCCCACAGTCTCCA	60	430	23	M57399
E3-Ubiquitin Ligase	UBE3-Lig	CAGGAATGGTTGTATCTCTTGTC	53	469	25	AY014180
E3-Ubiquitin Ligase	UBE3-Lig	AATGCCTCGTAAAAATCTCCAGTT	53	469	25	AY014180
aB-crystallin	aB	AGCCGCTCTTTGACCAGTCTTTC	60	452	18	NM_001885
aB-crystallin	aB	GCGGTGACAGCAGGCTTCTCTTC	60	452	18	NM_001885
Catalase	Cat	TACCCTCCTGGACTTTTTACATC	52	541	25	NM_001752
Catalase	Cat	CCTCATTCAGCAGTTTACATAGA	52	541	25	NM_001752
Metal-responsive Transcription Factor 1	MTF-1	GGGCCAGGACCTCAGCACAAT	59	445	25	XM_001412
Metal-responsive Transcription Factor 1	MTF-1	AGAAGCCCCAGCAACAACAGAAAG	59	445	25	XM_001412

The table lists the sequences, GenBank accession numbers, annealing temperatures, product lengths, and PCR cycle numbers for all gene-specific primers used in this study.

pairs)], where PM and MM denote perfect-match and mismatch probes, respectively. Each reported gene value represents the average signal intensity of 10 separately hybridized gene signatures. Any gene whose MM value was saturated or fell within τ distance of the PM value was excluded from the analysis. τ is a parameter used in performing the One-Sided Wilcoxon's Signed Rank test for the detection call and represents a threshold that the discrimination score for a probe set must exceed in order for a gene to be regarded as being present in the sample. Each gene was then assigned a call of Present (P), meaning that its intensity value is statistically greater than that of the background level and/or falls outside of the calculated τ distance, or Absent (A) meaning that its intensity value is not statistically greater than that of the background level and/or falls within the calculated τ distance. All of the genes described in this study are rated as present in at least one, if not both, of the cataract and clear lens samples. Any gene that was determined to be absent in both the cataract and clear lens samples was excluded from this report.

The microarray data were normalized using the Microarray Suite 5.0 software (Affymetrix) by multiplying the output of the experimental array by a Normalization Factor so that its average intensity is the same as that of the baseline array. The Microarray Suite 5.0 software also requires scaling, in which the output of any array is multiplied by a scaling factor to make its average intensity equal to a defined target intensity. For these studies a standard target intensity of 250 was used.

Semi-quantitative RT-PCR confirmation: Seventeen genes were selected for use in semi-quantitative RT-PCR con-

firmations of the hybridization results. Gene-specific primers were designed using the BLAST program and GenBank database (National Center for Biotechnology Information, Bethesda, MD). All primers were designed to cross intron/exon boundaries. The primer sequences, GenBank accession numbers, annealing temperatures, product lengths, and PCR cycle numbers for all gene-specific primers used in this study are indicated in Table 1. Semi-quantitative RT-PCR was performed using 50 ng of RNA with a commercial RT-PCR system used in accordance with the manufacturer's protocol (One-Step; Invitrogen, Gaithersburg, MD). To provide further confidence in the data and to show that the PCR reactions are within the linear range of PCR cycles, 3 control genes, catalase, metal-responsive transcription factor 1 (MTF-1), and α B-crystallin, and two genes of interest, HSP27-1 and -2 were evaluated by RT-PCR using 50 ng of cataract RNA and 5 different amounts (5, 10, 30, 50, and 100 ng) of clear lens RNA. Products were separated by gel electrophoresis on 1.5% agarose gels and visualized by ethidium bromide staining. Product formation for indicated genes was linear over all of the PCR cycles used. All PCR products were sequenced to ensure product authenticity. All gels were scanned and the percent adjusted volume intensities of all of the RT-PCR products were determined using a Biorad gel documentation system (Biorad, Hercules, CA). These values were used to calculate the approximate fold changes of the selected genes between cataract and clear lens epithelia.

Functional clustering and over-representation analysis of differentially expressed genes: Genes identified to be differentially expressed by 2 fold or greater according to the

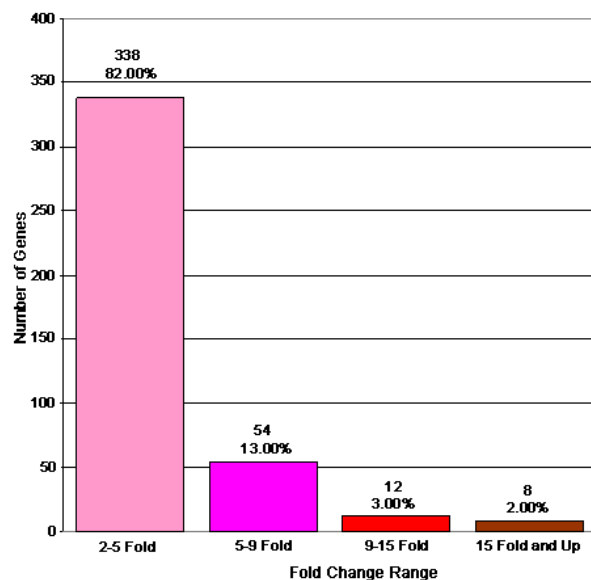


Figure 1. Genes increased 2 fold or greater between cataract and clear lenses. This figure graphically represents the genes whose expression levels are increased by 2 fold or greater in cataract relative to clear lenses. The total number of genes included in each fold change category are indicated. Percentages indicate the total number of genes in each category relative to the total number of increased genes (412) on the chip.

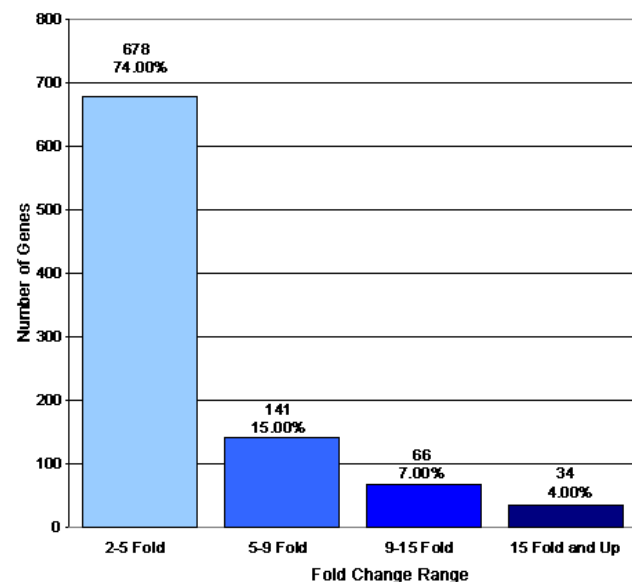


Figure 2. Genes decreased 2 fold or greater between cataract and clear lenses. This figure graphically represents the genes whose expression levels are decreased by 2 fold or greater in cataract relative to clear lenses. The total number of genes included in each fold change category are indicated. Percentages indicate the total number of genes in each category relative to the total number of decreased genes (919) on the chip.

microarray analysis were analyzed for significant functional clusters of genes using the EASE bioinformatics software package. This software package was used to rank functional clusters by statistical over-representation of individual genes in specific categories relative to all genes in the same category on the microarray. The functional clusters used by EASE were derived from the classification systems of the Gene Ontology,

Proteome's "At A Glance," SwissProt keywords, and Interpro protein domains.

RESULTS

Oligonucleotide microarray analysis: Analysis of gene expression differences between pooled age-matched cataract and

TABLE 2. GENES EXHIBITING DIFFERENTIAL EXPRESSION IN CATARACT RELATIVE TO CLEAR LENSES

Genes exhibiting increased expression in cataract relative to clear lenses

Gene name	Accession number	Normal signal intensity	Cataract signal intensity	Fold
nuclear phosphoprotein	BE796924	348.8 (P)	1730.7 (P)	5.28
di-N-acetyl-chitobiase	NM_004388	117.2 (A)	322.9 (P)	5.28
Hypothetical protein FLJ21551	NM_024801	121 (P)	524.5 (P)	5.28
Hypothetical protein PRO1048	NM_018497	29.3 (A)	261.1 (P)	5.28
EST	AA972711	354.7 (P)	1919.5 (P)	5.28
Human erythroid-specific transcription factor EKLF	U65404	70.3 (P)	408.9 (P)	5.28
Chromosome 14 clone	AC007956	154.4 (P)	649.3 (P)	5.66
tetratricopeptide repeat domain 3	AW510696	431.9 (P)	1752.4 (P)	5.66
Hypothetical protein FLJ11827	NM_025093	58.5 (A)	338.9 (P)	5.66
ubiquitin 1	T70262	397.9 (P)	1981.9 (P)	5.66
alpha thalassemia mental retardation syndrome X-linked	AI650257	154.9 (P)	852.1 (P)	5.66
Neuron-specific protein	NM_014392	54.5 (A)	338.2 (P)	5.66
growth factor receptor-bound protein 10	D86962	126.6 (P)	544.2 (P)	5.66
Disabled homolog 2 (mitogen-responsive phosphoprotein)	NM_001343	237 (P)	1096.6 (P)	6.06
Secreted apoptosis related protein 2 (SARP2)	AF017987	473.2 (P)	3068.6 (P)	6.06
acid sphingomyelinase-like phosphodiesterase	AA873600	48.7 (A)	264.1 (P)	6.06
EST	AI694562	2039.8 (P)	14553.9 (P)	6.06
KIAA1641 protein	NM_025190	178.7 (P)	878.1 (P)	6.06
Tryptophan 2,3-dioxygenase	NM_005651	37.4 (A)	324.8 (P)	6.06
adducin 3 (gamma)	AI763123	100.8 (A)	379.3 (P)	6.06
Type II Golgi membrane protein	NM_014498	100 (A)	618.9 (P)	6.06
EST	AA634446	13.3 (A)	137.2 (P)	6.5
Na ⁺ /H ⁺ exchanger isoform 2	AF073299	133.9 (A)	1443.4 (P)	6.5
Ser-Thr protein kinase	NM_003607	1015.2 (P)	3771 (P)	6.5
Sjogren syndrome antigen B	BG532929	47.8 (A)	374.3 (P)	6.5
clone COL05464	AK025143	68.1 (A)	571.6 (P)	6.5
EST	BF592782	479.5 (P)	3072.6 (P)	6.5
Bcl-2-associated transcription factor short form mRNA	AF249273	94.5 (P)	518.1 (P)	6.5
eukaryotic translation initiation factor 4 gamma	BE966878	112.4 (P)	612.6 (P)	6.5
Nijmegen breakage syndrome 1 (nibrin)	AI796269	83.6 (A)	1188 (P)	6.96
DEADH (Asp-Glu-Ala-AspHis) box polypeptide 17	AW188131	153.2 (A)	1396 (P)	6.96
KIAA0876 protein	AW237172	128.9 (A)	1181.2 (P)	6.96
Arginine methyltransferase	U79286	62.8 (A)	366.1 (P)	6.96
Small nuclear RNA activating complex, polypeptide 1, 43 kD (SNAPC1)	NM_003082	145.6 (P)	643.5 (P)	6.96
Zinc finger protein 161 (ZNF161)	NM_007146	81.9 (A)	446.7 (P)	6.96
KIAA1641 protein	AB046861	32 (A)	201.3 (P)	6.96
copine III	AA541758	96.6 (A)	775.4 (P)	6.96
natural killer-tumor recognition sequence	AI361805	398.2 (P)	2412.8 (P)	6.96
KIAA0480 gene product	AW299294	154 (P)	997.5 (P)	7.46
Nerve growth factor (HBNF-1)	M57399	1448.1 (P)	7425.6 (P)	7.46
natural killer-tumor recognition sequence	AI688640	95.4 (P)	829 (P)	7.46
pleiophin	BC005916	1187.8 (P)	10502.3 (P)	7.46
nuclear receptor interacting protein 1	AI824012	58.3 (A)	383.9 (P)	7.46
EST	AW293343	84.3 (P)	630.2 (P)	7.46
ATPase, Na ⁺ /K ⁺ transporting, beta 1 polypeptide	BC000006	1233.8 (P)	14152 (P)	8
Glutathione peroxidase 2	NM_002083	31.7 (A)	257.1 (P)	8
transformer-2 alpha	AW978896	97 (A)	618.3 (P)	8
Tubby like protein 1	NM_003322	27.3 (A)	211.3 (P)	8
EST	BF448315	197.7 (P)	1500.5 (P)	8

TABLE 2. CONTINUED.

Genes exhibiting increased expression in cataract relative to clear lenses

DNA for HBV integration sites	X04014	80.7 (A)	607.8 (P)	8
similar to widely-interspaced zinc finger motifs	AI828531	34.6 (A)	273.6 (P)	8
cDNA DKFZp566M043	AL050065	36.2 (A)	322.8 (P)	8.57
secretory carrier membrane protein 1	BF058944	177.3 (P)	928.9 (P)	8.57
chondroitin sulfate proteoglycan 6 (bamacan)	AI373676	71.3 (P)	1010.3 (P)	8.57
KIAA0594 protein	AW183677	39.1 (A)	404.7 (P)	9.19
Claudin 1 (CLDN1)	NM_021101	41 (A)	268.1 (P)	9.85
KIAA0256 gene product	N52532	71.7 (A)	1709.6 (P)	9.85
HRIHFB2017	AB015331	64.1 (A)	368.4 (P)	9.85
KIAA0888 protein	AB020695	173.8 (A)	2224.6 (P)	10.56
Osteomodulin	AI765819	26.4 (A)	351.8 (P)	11.31
Bicaudal-D (BICD)	U90030	40.8 (A)	888.1 (P)	12.13
EST	AI278204	46.2 (A)	331.8 (P)	12.13
cDNA: FLJ21198	AK024851	13.5 (A)	217.6 (P)	12.13
KIAA0447 gene product	BE885244	45.2 (A)	664 (P)	13
chloride channel 3	AA902971	25.7 (A)	221.7 (P)	14.93
Wiskott-Aldrich syndrome-like	BE504979	51.4 (A)	686 (P)	14.93
Cofactor required for Sp1 transcriptional activation, subunit 2	NM_004229	9.2 (A)	196.8 (P)	16
KIAA0494 gene product	BC002525	15.5 (A)	419.6 (P)	17.15
ring finger protein 15	AU157590	62.5 (A)	719.2 (P)	19.7
myeloidlymphoid or mixed-lineage leukemia	AA715041	39.2 (A)	518.1 (P)	19.7
PRO2667	AF119889	31.3 (A)	717.7 (P)	19.7
cDNA DKFZp564M2422	AL050388	4.2 (A)	185.4 (P)	19.7
Similar to histamine N-methyltransferase	BC005907	10.4 (A)	308 (P)	27.86
Testis-specific XK-related protein on Y	NM_004677	4.3 (A)	124.2 (P)	32

Genes exhibiting decreased expression in cataract relative to clear lenses

Gene name	Accession number	Normal signal intensity	Cataract signal intensity	Fold
Jagged 1	U73936	916.3 (P)	69.9 (A)	5.28
Ribosomal protein, large, P0	NM_001002	14191.2 (P)	3138.4 (P)	5.28
Fibrillin 1	NM_000138	404.2 (P)	55.2 (A)	5.28
Similar to eukaryotic translation initiation factor 4A, isoform 1	BC006210	2672.3 (P)	494.9 (A)	5.28
EST	AI799802	228.4 (P)	23.1 (A)	5.28
Zinc finger protein 219	NM_016423	300.2 (P)	53.3 (A)	5.28
Similar to eukaryotic translation initiation factor 3, subunit 8	BC000533	2697.1 (P)	471.5 (P)	5.28
heat shock cognate protein 54	AB034951	1342.6 (P)	152 (A)	5.28
Pyruvate kinase, muscle	NM_002654	1098.2 (P)	221.9 (A)	5.28
IMP (inosine monophosphate) dehydrogenase 2	NM_000884	1011.6 (P)	124.8 (A)	5.28
EST	AI816291	458.9 (P)	66.1 (A)	5.28
Translocase of inner mitochondrial membrane 23 homolog	NM_006327	435.6 (P)	86.5 (A)	5.28
4-hydroxyphenylpruvate dioxygenase	NM_002150	206.7 (P)	36.9 (A)	5.28
Heat shock 27 kD protein 2	NM_001541	1056.5 (P)	172.3 (A)	5.28
Carbonyl reductase 1	BC002511	589.2 (P)	27.6 (A)	5.28
Proteasome (prosome, macropain) subunit, beta type, 4	NM_002796	875.3 (P)	143 (A)	5.28
Small membrane protein 1	NM_014313	502 (P)	78.7 (A)	5.28
Fatty acid binding protein 3, muscle and heart (mammary-derived growth inhibitor)	NM_004102	244 (P)	48.2 (A)	5.28
Calpastatin	AF327443	300.3 (P)	81.1 (A)	5.28
Myosin, light polypeptide, regulatory, non-sarcomeric	NM_006471	3899.8 (P)	876.3 (P)	5.28
Proteolipid protein 2 (colonic epithelium-enriched)	NM_002668	437.4 (P)	50.8 (A)	5.28
ribosomal protein L4	AI953886	6333.2 (P)	716.8 (P)	5.28
cDNA DKFZp586D1122	AL050166	199.2 (P)	29.6 (A)	5.28
poly(rC)-binding protein 2	NM_005016	1855.1 (P)	204.4 (A)	5.28
Metallothionein If gene	M10943	5381.9 (P)	776.9 (A)	5.66

TABLE 2. CONTINUED.

Genes exhibiting decreased expression in cataract relative to clear lenses

3-hydroxy-3-methylglutaryl-Coenzyme A reductase	AL518627	159.3 (P)	30.3 (A)	5.66
G8 protein	NM_016947	3539.8 (P)	558.7 (P)	5.66
SMX5-like protein	AF196468	358.8 (P)	39.1 (A)	5.66
Microtubule-associated proteins 1A1B light chain 3	AF183417	423.7 (P)	79.3 (A)	5.66
PRO2640	AF116710	8064.3 (P)	991.9 (P)	5.66
MYLE protein	NM_014015	471 (P)	52.6 (A)	5.66
Cold shock domain protein A	NM_003651	1098.3 (P)	144.3 (A)	5.66
kinesin 2	AA284075	236.3 (P)	40.9 (A)	5.66
Cell membrane glycoprotein	NM_007002	368.8 (P)	75.1 (A)	5.66
Biliverdin reductase	NM_000713	1583.4 (P)	498.1 (P)	5.66
Nuclear localization signal deleted in velocardiofacial syndrome	NM_003776	970.5 (P)	125.9 (A)	5.66
clone RP11-48602	AL356115	10470 (P)	1310.9 (P)	5.66
proteasome (prosome, macropain) subunit, alpha type, 3	NM_002788	452 (P)	46 (A)	5.66
Cyclin D1	BC000076	182.7 (P)	21.7 (A)	5.66
Heat shock 70 kD protein 1B	NM_005346	1660.9 (P)	397.7 (P)	5.66
CD24 signal transducer	L33930	736.9 (P)	187.1 (A)	5.66
Zyxin related protein ZRP-1	AF000974	792.4 (P)	113.6 (A)	5.66
solute carrier family 2 (facilitated glucose transporter), member 3	BE550486	210.6 (P)	76.2 (A)	5.66
Tubulin, beta 5	BC005838	3024.6 (P)	533.4 (M)	5.66
weakly similar to LONGEVIY-ASSURANCE PROTEIN 1	AK001105	1037.6 (P)	178.7 (A)	5.66
clone 1033B10	AL031228	565 (P)	92 (A)	6.06
S-adenosylhomocysteine hydrolase (AHCY)	NM_000687	365.9 (P)	59.1 (A)	6.06
ribosomal protein, large, P0	AI953822	8792.1 (P)	1133.5 (P)	6.06
Ovarian beta-A inhibin	M13436	6485.9 (P)	898.3 (P)	6.06
MYG1 protein	NM_021640	583.2 (P)	103.9 (A)	6.06
ribosomal protein L13	AI186735	7108.6 (P)	1468.8 (P)	6.06
Splicing factor arginineserine-rich 9	NM_003769	1438.8 (P)	422.6 (A)	6.06
HDCMB21P gene	AF072098	10344.7 (P)	699.8 (P)	6.06
Goliath protein	NM_018434	340.6 (P)	28.8 (A)	6.06
Eukaryotic translation initiation factor 2B, subunit 1 (alpha, 26 kD)	NM_001414	281.1 (P)	54.1 (A)	6.06
ribosomal protein L13	AW574664	3994.8 (P)	371.4 (A)	6.06
Proteasome (prosome, macropain) subunit, beta type, 7	NM_002799	2050 (P)	332.4 (M)	6.06
Tubulin, beta, 2	BC004188	1084.5 (P)	202.4 (A)	6.06
Phosphatidylethanolamine N-methyltransferase	NM_007169	670.3 (P)	47.1 (A)	6.06
Adaptor-related protein complex 2, mu 1 subunit	NM_004068	863.9 (P)	165.4 (A)	6.06
cDNA DKFZp564B076	AL049313	470.2 (P)	52.3 (A)	6.06
clone RP4-781L3	AL121994	897.8 (P)	150.3 (A)	6.06
Alpha-actinin-2 associated LIM protein mRNA, alternatively spliced product	AF002280	189.4 (P)	28.7 (A)	6.06
Threonyl-tRNA synthetase	NM_003191	958 (P)	97.8 (A)	6.06
MCP-1=monocyte chemotactic protein human, aortic endothelial cells	S69738	771 (P)	73 (A)	6.5
eukaryotic translation elongation factor 1 gamma	BE963164	13185.4 (P)	1579.7 (A)	6.5
Lectin, galactoside-binding, soluble, 1(galectin1)	NM_002305	2609.9 (P)	94.5 (A)	6.5
CGI-44 protein; sulfide dehydrogenase like	NM_021199	1703.9 (P)	151.3 (A)	6.5
DnaJ (Hsp40) homolog, subfamily B, member 1	BG537255	532.8 (P)	77.4 (A)	6.5
Fragile histidine triad gene	HN_002012	341.8 (P)	59.8 (A)	6.5
Carboxypeptidase B1	NM_001871	337.8 (P)	35.4 (A)	6.5
Crystallin, beta B2	NM_000496	20885.8 (P)	3332.7 (P)	6.5
Meiotic recombination protein REC14	AF309553	134.4 (P)	34.9 (A)	6.5
Selenoprotein W, 1	NM_003009	707.1 (P)	39.3 (A)	6.5
mRNA for hMBF1alpha	AB002282	2012.1 (P)	211.9 (A)	6.5
tudor repeat associator with PCTAIRE 2	AW129593	2669.4 (P)	387.8 (M)	6.5
EST	AV705559	593.1 (P)	107.4 (A)	6.5
Clone: SMAP31-12	AB059408	483.7 (P)	68.1 (A)	6.5
Growth arrest and DNA damage inducible proteinbeta	AF087853	1895.6 (P)	39.3 (A)	6.5
Crystallin, gamma B	NM_005210	721 (P)	104.8 (A)	6.5
Eukaryotic translation elongation factor 1 delta (guanine nucleotide exchange protein)	NM_001960	3814.7 (P)	480.1 (A)	6.5
FK506-binding protein 2	NM_004470	503.6 (P)	17.5 (A)	6.5
HLA class II region expressed gene KE2	NM_014260	382.3 (P)	30.3 (A)	6.5
Neuronal cell adhesion molecule	NM_005010	613.1 (P)	94.8 (A)	6.5
polymerase (RNA) II (DNA directed) polypeptide J	BG335629	552.8 (P)	31.8 (A)	6.5
Ribosomal protein L27a	NM_000990	12053.7 (P)	1609.9 (P)	6.5

TABLE 2. CONTINUED.

Genes exhibiting decreased expression in cataract relative to clear lenses

EST	L43577	354.2 (P)	43 (A)	6.96
Tetraspan 3	NM_005724	183 (P)	21.3 (A)	6.96
phosphoserine aminotransferase	AI889380	4608.5 (P)	970.4 (P)	6.96
Nuclear prelamin A recognition factor	NM_012336	482 (P)	58.2 (A)	6.96
Zinc finger protein homologous to Zfp-36 in mouse	NM_003407	651.1 (P)	63.6 (A)	6.96
cDNA DKFZp564J1516	AL136601	192.2 (P)	30.5 (A)	6.96
Antizyme inhibitor	NM_015878	232.8 (P)	25.5 (A)	6.96
G protein-coupled receptor 39	AL567376	257 (P)	63.1 (A)	6.96
prostatic binding protein	BE969671	3392.7 (P)	310.4 (P)	6.96
Tetratricopeptide repeat domain 2	NM_0003315	397.2 (P)	43.4 (A)	6.96
Ribosomal protein S15	NM_001018	15776.8 (P)	2287.8 (P)	6.96
Hypothetical protein FLJ11730	NM_022756	639.3 (P)	105.1 (A)	6.96
kinesin 2	AA284075	199.9 (P)	21.7 (A)	6.96
Prefoldin 5	NM_002624	2490.6 (P)	261.6 (A)	6.96
Poly(A)-binding protein, cytoplasmic 4 (inducible form)	NM_003819	437.9 (P)	32.9 (A)	6.96
Ribosomal protein L35	NM_007209	6130.5 (P)	732.7 (P)	6.96
Catenin (cadherin-associated protein), alpha 2	NM_004389	350.7 (P)	28.5 (A)	6.96
Hypothetical protein FLJ10493	NM_018112	107.9 (P)	17.8 (A)	6.96
Lysosomal-associated membrane protein 1	NM_005561	888.3 (P)	54.1 (A)	6.96
Human growth hormone-dependent insulin-like growth factor-binding protein	M31159	2003.6 (P)	285.9 (P)	6.96
glutathione peroxidase 3	AW149846	5548.5 (P)	521 (P)	6.96
Prostatic binding protein	NM_002567	4056.2 (P)	356.9 (A)	7.46
GMPR2 for guanosine monophosphate reductase isolog	NM_016576	584.3 (P)	38.3 (A)	7.46
hemoglobin, alpha 1	T50399	427.5 (P)	75.7 (A)	7.46
Ribosomal protein L8	NM_000973	5766.6 (P)	462.4 (A)	7.46
F-box protein FLR1	AF142481	771.2 (P)	114.6 (A)	7.46
Homo sapiens, Similar to tubulin, beta, 4	BC002654	1096.5 (P)	127.3 (A)	7.46
Ribosomal protein L29	NM_000992	1889.9 (P)	228.7 (A)	7.46
KIAA0874 protein	AB020681	249.4 (P)	45.6 (A)	7.46
CGI-91 protein	NM_016034	327.1 (P)	49.7 (A)	7.46
Pre-mRNA splicing factor 2 p32 subunit	L04636	518.2 (P)	46.5 (A)	7.46
Phosphoglycerate kinase 1	NM_000291	2262.5 (P)	332.5 (P)	7.46
Human 28S rRNA sequence	M11167	3708.3 (P)	648.4 (P)	7.46
Similar to granulin	BC000324	480 (P)	65.7 (A)	8
hypothetical protein FLJ10698	AI951798	422.6 (P)	49 (A)	8
solute carrier family 25 (mitochondrial carrier; adenine nucleotide translocator), member 6	AI961224	6069.8 (P)	397.1 (A)	8
SKIP for skeletal muscle and kidney enriched	AI806031	30.6 (A)	249.4	8
inositol phosphatase				
Protein kinase	AF133207	2162.2 (P)	316 (A)	8
Extracellular matrix protein 1	U65932	1252.6 (P)	150.3 (A)	8
Alpha II spectrin	U83867	843.9 (P)	96.5 (A)	8
nucleophosminB23.2	AB042278	655 (P)	70.7 (A)	8
Ribosomal protein L4	NM_000968	7153.3 (P)	854.4 (P)	8
Phosphatidylcholine transfer protein	NM_021213	205 (P)	23.8 (A)	8
SEC13 (S. cerevisiae)-like 1	NM_030673	420.4 (P)	37.6 (A)	8
Homo sapiens mRNA for puromycin sensitive aminopeptidase	AJ132583	303.3 (P)	39.2 (A)	8
Eukaryotic translation initiation factor 3, subunit 4 (delta, 44 kD)	BC000733	1480 (P)	131.3 (A)	8
SET translocation (myeloid leukemia-associated)	AI278616	459 (P)	35.1 (A)	8
PRO1608	AF119850	10333.9 (P)	1251.4 (P)	8
Human bcl-1 mRNA	M73554	780.7 (P)	139.7 (A)	8.57
ECSIT	NM_016581	238.5 (P)	27.4 (A)	8.57
MCT-1 protein	NM_014060	328.5 (P)	20.5 (A)	8.57
Human soluble protein Jagged mRNA	U77914	1063.3 (P)	109.4 (A)	8.57
nidogen (enactin)	BF940043	608.8 (P)	93.6 (A)	8.57
Mitochondrial ribosomal protein S15	NM_031280	132.4 (P)	11.3 (A)	8.57
Proteasome (prosome, macropain) subunit, beta type, 1	NM_002793	1915.3 (P)	357.2 (A)	8.57
Translocase of inner mitochondrial membrane 17 (yeast) homolog A	BC004439	128.3 (P)	7.6 (A)	9.19
Microfibrillar-associated protein 2, transcript variant 1	NM_017459	233.4 (P)	23.6 (A)	9.19
Ribosomal protein L4	BC005817	7644.3 (P)	816.1 (P)	9.19
Zinc finger protein 162	NM_004630	734.7 (P)	25.1 (A)	9.19
Tyrosine 3-monooxygenasetryptophan 5-monooxygenase	BC003623	373.6 (P)	32.5 (A)	9.19

TABLE 2. CONTINUED.

Genes exhibiting decreased expression in cataract relative to clear lenses

activation protein, zeta polypeptide				
Spinde pole body protein	NM_006322	215.4 (P)	12.6 (A)	9.19
Glycogenin	NM_004130	407 (P)	30.8 (A)	9.85
6-pyruvoyl-tetrahydropterin synthasedimerization cofactor of hepatocyte nuclear factor alpha	NM_000281	217.7 (P)	13.4 (A)	9.85
Moesin	NM_002444	974.5 (P)	38.7 (A)	9.85
Nuclear autoantigenic sperm protein (histone-binding)	NM_002482	155.1 (P)	16.4 (A)	9.85
Metalloprotease	NM_007038	220.2 (P)	9.9 (A)	9.85
KIAA0116 protein	AL581473	822.7 (P)	45.9 (A)	9.85
GAPDH	M33197	5091.6 (P)	530.9 (A)	9.85
Brain acid-soluble protein 1	NM_006317	7329.2 (P)	674 (P)	9.85
HSPC177	NM_016410	310.9 (P)	30.8 (A)	9.85
glyceraldehyde-3-phosphate dehydrogenase	BF689355	9541.6 (P)	1048.9 (P)	9.85
Latent transforming growth factor beta binding protein 3	NM_021070	377.9 (P)	39 (A)	9.85
U6 snRNA-associated Sm-like protein LSm7	NM_016199	395.4 (P)	37 (A)	10.56
GANP protein	AJ010089	462.1 (P)	29.2 (A)	10.56
McKusick-Kaufman syndrome protein	NM_018848	533.2 (P)	20.9 (A)	10.56
Clone image:3611719	BC003542	167 (P)	22.2 (A)	10.56
Cyclin G1	BC000196	4919.8 (P)	480.8 (A)	10.56
Microtubule associated protein	AI633566	402.3 (P)	44.9 (A)	10.56
MM-1 beta	AB055804	1917.7 (P)	106.5 (A)	10.56
transketolase	L12711	5334 (P)	535.8 (P)	10.56
78 kDa gastrin-binding protein	U04627	370.5 (P)	24.3 (A)	10.56
SH3 domain binding glutamic acid-rich protein	NM_007341	682.4 (P)	38.7 (A)	10.56
EEF1 gamma	NM_001404	9570.8 (P)	935.6 (A)	10.56
phospholipase C, beta 3	BE305165	419.7 (P)	42.3 (A)	10.56
Glutathione peroxidase 3	NM_002084	9749.5 (P)	594.4 (P)	11.31
RD protein	L03411	506.3 (P)	40.5 (A)	11.31
Adaptor-related protein complex 2	NM_021575	225 (P)	19.3 (A)	11.31
Phosphomannomutase 1	NM_002676	238.4 (P)	40.7 (A)	11.31
Quinone oxidoreductase homolog	BC000474	934 (P)	50.2 (A)	11.31
HSPC034 protein	NM_016126	217.9 (P)	12.8 (A)	11.31
Ornithin decarboxylase antizyme 1	AF090094	1153.7 (P)	36.4 (A)	11.31
JM5 protein	BC000464	327.3 (P)	30.5 (A)	12.13
Retinitis pigmentosa 2	NM_006915	33.1 (P)	1.3 (A)	12.13
Guanine nucleotide binding protein (G protein), beta polypeptide 2-like 1	NM_006098	3013.5 (P)	315.4 (A)	12.13
Cytidine deaminase	NM_001785	324.7 (P)	23.4 (A)	12.13
alpha-2-HS-glycoprotein	BG538564	3032.1 (P)	152.1 (A)	12.13
Ribosomal protein L11	NM_000975	4539.6 (P)	162.2 (A)	12.13
L-iditol-2 dehydrogenase	L29008	1540.6 (P)	93.4 (A)	12.13
v-fos FBJ murine osteosarcoma viral oncogene homolog	BC004490	508.5 (P)	17.2 (A)	12.13
Crystallin beta B2	NM_000496	18394.2 (P)	1113.3 (P)	12.13
28S ribosomal RNA gene	M27830	8810.6 (P)	639.5 (P)	12.13
KIAA0230 gene	D86983	300.7 (P)	19.7 (A)	12.13
Clone 24461	AF070577	517.8 (P)	16.7 (A)	12.13
MRJ gene for a member of the DNAJ protein family	BC002446	244.5 (P)	19 (A)	13
HMG box mRNA, 3 end cds.	L07335	1053.5 (P)	80.1 (A)	13
Beaded filament structural protein 2, phakinin	NM_003571	7986.8 (P)	454.7 (A)	13
Adipose specific 2	NM_006829	822.3 (P)	103.3 (A)	13
NADH dehydrogenase (ubiquitone) 1 alpha subcomplex, 7	NM_005001	537 (P)	24 (A)	13
Histidyl-tRNA synthetase	NM_002109	1033.2 (P)	33.8 (A)	13
Myristoylated alanine-rich protein kinase C substrate	NM_002356	203.9 (P)	22.5 (A)	13.93
Id-2H complete cds. inhibitor of DNA binding 2, dominant negative helix-loop-helix protein	D13891	195.8 (P)	16.8 (A)	13.93
Ancient ubiquitous protein 1	NM_012103	258.7 (P)	25.4 (A)	13.93
solute carrier family 1 (glutamate/neutral amino acid transporter), member 4	BF340083	5269.5 (P)	333.4 (P)	13.93
signal peptidase complex	N99438	789.3 (P)	51.9 (A)	13.93
ID4 helix-loop-helix DNA binding protein	AL022726	210.3 (P)	16.1 (A)	14.93
proteasome (prosome, macropain) inhibitor subunit1	BG029917	426.1 (P)	28.4 (A)	14.93
Cysteine-rich protein 1 (intestinal)	NM_001311	583 (P)	31 (A)	14.93
Epithelial membrane protein 1	NM_001423	154.2 (P)	10.6 (A)	14.93
EST	R06655	758.5 (P)	32 (A)	14.93

TABLE 2. CONTINUED.

Genes exhibiting decreased expression in cataract relative to clear lenses

Heterogeneous nuclear ribonucleoprotein AB	NM_004499	638.7 (P)	33.7 (A)	14.93
HIV-1 TAR RNA binding protein	L22453	4646.4 (P)	263 (A)	14.93
Calpain 4, small subunit (30 kDa)	NM_001749	866.5 (P)	44.7 (A)	16
Archain 1	NM_001655	635.5 (P)	12.6 (A)	16
RuvB (E coli homolog)-like 2	NM_006666	451.2 (P)	31.5 (A)	16
peptidylprolyl isomerase B (cyclophilin B)	NM_000942	741.1 (P)	24.4 (A)	17.15
Beaded filament structural protein 1, filensin	NM_001195	6597.1 (P)	185.7 (A)	17.15
HSPC165 protein	NM_014185	393.4 (P)	22.3 (A)	17.15
chimerin (chimaerin) 1	BF339445	709.7 (P)	44.2 (A)	17.15
Hypothetical protein FLJ11798	NM_024907	510.9 (P)	16.8 (A)	18.38
Saposin proteins A-D	M32221	554.2 (P)	25.1 (A)	18.38
Uncharacterized hematopoietic stemprogenitor cells protein MDS032	NM_018467	335.2 (P)	25 (A)	19.7
Eukaryotic translation elongtion factor 2	NM_001961	4841 (P)	138.5 (A)	21.11
Lysyl oxidase-like 1	NM_005576	824.8 (P)	18.7 (A)	21.11
transketolase	BF696840	1557.5 (P)	27 (A)	22.63
Alpha A crystallin	U66584	10945.8 (P)	264.4 (P)	22.63
Crystallin beta B3	NM_004076	2515.8 (P)	64.9 (A)	22.63
glycoprotein M6A	BF939489	360.8 (P)	19.6 (A)	24.25
Growth arrest and DNA-damage-inducible, alpha	NM_001924	1548.3 (P)	31 (A)	24.25
pUb-R5	AB033605	867 (P)	30 (A)	24.25
solute carrier family 25 (mitochondrial carrier; adenine nucleotide translocator), member 6	AA916851	1736.5 (P)	20.8 (A)	25.99
ribosomal protein, large, P0	AA555113	2885.2 (P)	73.5 (A)	27.86
Lens intrinsic membrane protein 2	NM_030657	7106.4 (P)	144.3 (A)	27.86
Crystallin beta A3	NM_005208	16082.8 (P)	582.6 (M)	27.86
Microvascular endothelial differentiation gene 1	NM_012328	110.3 (P)	6.4 (A)	27.86
Crystallin gamma D	NM_006891	6226.2 (P)	204.5 (A)	29.86
Ribosomal protein S9	NM_001013	5469.9 (P)	207.3 (A)	32
Phosphoglycerate kinase	S81916	477.3 (P)	23.8 (A)	42.22
matrix Gla protein	AI653730	546.9 (P)	14.5 (A)	42.22
Intersectin short isoform	AF114488	119.3 (P)	4.3 (A)	45.25
Hypothetical protein PRO2577	NM_018630	133.3 (P)	6.8 (A)	45.25
Lengsin	NM_016571	2135 (P)	17.1 (A)	51.98
Crystallin beta A2	NM_005209	14598.1 (P)	108.3 (A)	55.72
Crystallin beta B1	NM_001887	7181.6 (P)	68.5 (A)	119.43
Heat shock 27 kD protein 1	NM_001540	3620.6 (P)	28.2 (A)	128
Crystallin beta A4	NM_001886	17523.3 (P)	118.1 (A)	168.9

In the third and fourth columns, the abbreviations P is present, statistically greater than background intensity values, A is absent, not statistically different than background intensity values, and M is marginal, possibly different than background intensity values.

clear lenses was conducted using Affymetrix HG_U133A microarrays as described in the methods section. In this analysis, only one hybridization was conducted for each RNA population due to the extremely large number of human lens epithelia required for this type of analysis and the limited availability of these tissues. Comparison of the gene expression data for 22,215 genes represented by 222,830 separate probe sets, each probe set containing 10 perfect match and 10 1 base pair mismatch probe sequences, between cataract and clear lens samples, identified 412 transcripts that were increased (Figure 1) and 919 transcripts that were decreased (Figure 2) by 2 fold or greater in cataract compared to clear lenses. Of the genes that exhibited increased expression in cataracts, 82% of them were increased by 2-5 fold, 13% by 5-9 fold, 3% by 9-15 fold, and 2% by greater than 15 fold (Figure 1). Of the genes that exhibited decreased expression in cataracts, 74% of them fell into the 2-5 fold range, 15% in the 5-9 fold range, 7% in the 9-15 fold range, and 4% in the 15 fold and greater range (Figure 2). Of the identified genes, 74 exhibited increased expression, of which 24 are ESTs or unknown gene products,

and 241 exhibited decreased expression, of which 25 are ESTs or unknown gene products, at the 5 fold or greater level in cataract relative to clear lenses. These genes and their relative expression levels, intensity values and accession numbers are listed in Table 2. The raw microarray data, including intensity values and its statistical analysis, can be accessed in Appendix 1.

Semi-quantitative RT-PCR confirmation: In order to confirm the accuracy of the microarray data, semi-quantitative RT-PCR was conducted with the original RNA samples used for the microarray experiments and 2 other sets of separately prepared cataract and clear lens RNA samples. Thirteen genes that were either increased or decreased by 2 fold or greater in cataracts were first examined using the same RNA samples that were used for the microarray studies. These included Na⁺/H⁺ exchanger isoform II (6.50 fold), serine/threonine protein kinase (3.73 fold), Na⁺/K⁺ ATPase (8.00 fold), secreted apoptosis related protein 2 (6.06 fold), pleiotrophin (7.46 fold), and E3-ubiquitin ligase (4.59 fold) which all exhibited increased expression in cataracts according to the microarray

data. Heat shock protein 27-1 (128 fold), α A-crystallin (22.63 fold), ribosomal protein large subunit 13a (2.64 fold), metallothionein IF (5.66 fold), metallothionein IH (3.48 fold), metallothionein IG (3.73 fold), and glutathione peroxidase-1 (4.92 fold) all exhibited decreased expression in cataracts according to the microarray data.

Eleven of the 13 genes examined followed the same trends in gene expression as demonstrated by the microarray study (Figure 3A) using the original RNA samples including Na^+/H^+ exchanger isoform II, secreted apoptosis related protein 2, pleiotrophin, E3-ubiquitin ligase, heat shock protein 27-1, α A-crystallin, ribosomal protein large subunit 13a, metallothionein IF, metallothionein IH, metallothionein IG, and glutathione peroxidase-1. The two genes that did not follow the same trends in gene expression as demonstrated by the microarray data were serine/threonine protein kinase and Na^+/K^+ ATPase (Figure 3A).

A second sample of RNA was prepared from an additional 50 cataract and 10 age-matched clear lenses. Due to the limited amount of RNA recovered from the second population of cataracts, seven of the 13 aforementioned genes (including the two that did not confirm the microarray data using

the first samples of RNA) were re-examined using the new samples of RNA. Of these, five of the seven genes exhibited similar trends as detected in the microarray analysis including Na^+/H^+ exchanger isoform II, pleiotrophin, metallothionein IF, serine/threonine protein kinase, and Na^+/K^+ ATPase (Figure 3B). The two genes that did not reconfirm in the second sample of RNA were α A-crystallin and ribosomal protein large subunit 13a.

In order to further confirm the trends exhibited by the microarray study and to demonstrate that the PCR cycles used are within the linear range, we examined two particular genes of interest in a third sample of RNA prepared from another 50 cataract and 10 age-matched clear lenses. Consistent with the microarray data, Hsp 27 form 1 and 2 exhibited decreased expression in cataract relative to clear lenses using a fixed amount of cataract RNA (50 ng) and 5 different amounts of clear lens RNA (5, 10, 30, 50, and 100 ng, Figure 4). Heat

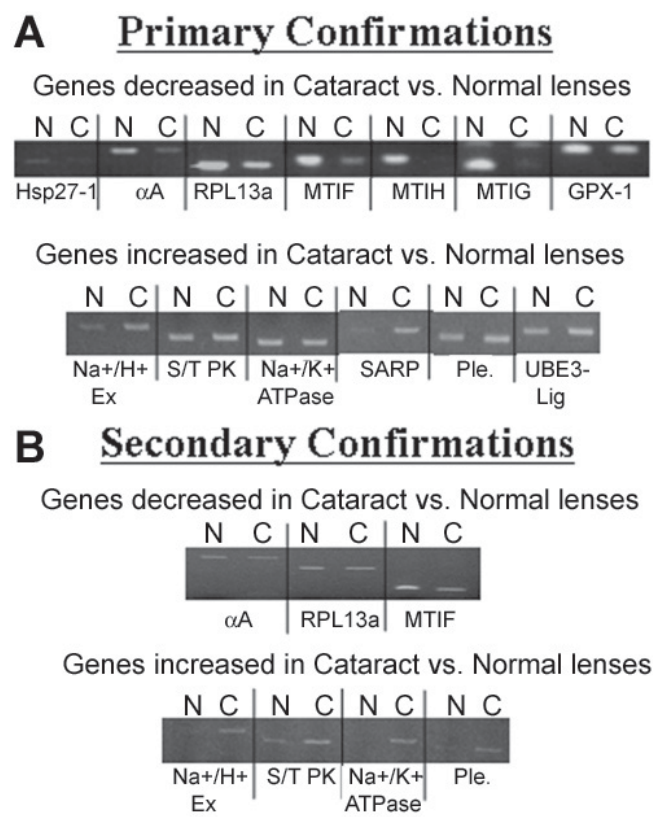


Figure 3. RT-PCR confirmation of gene expression differences. RT-PCR confirmation of gene expression differences detected by microarray hybridization between cataract (C) and normal (N) lens epithelia. The expression levels of indicated genes were confirmed by RT-PCR. **A:** Genes examined using the same cataract and clear lens RNAs analyzed by microarray hybridization. **B:** Genes examined using separately prepared cataract and clear lens RNA samples.

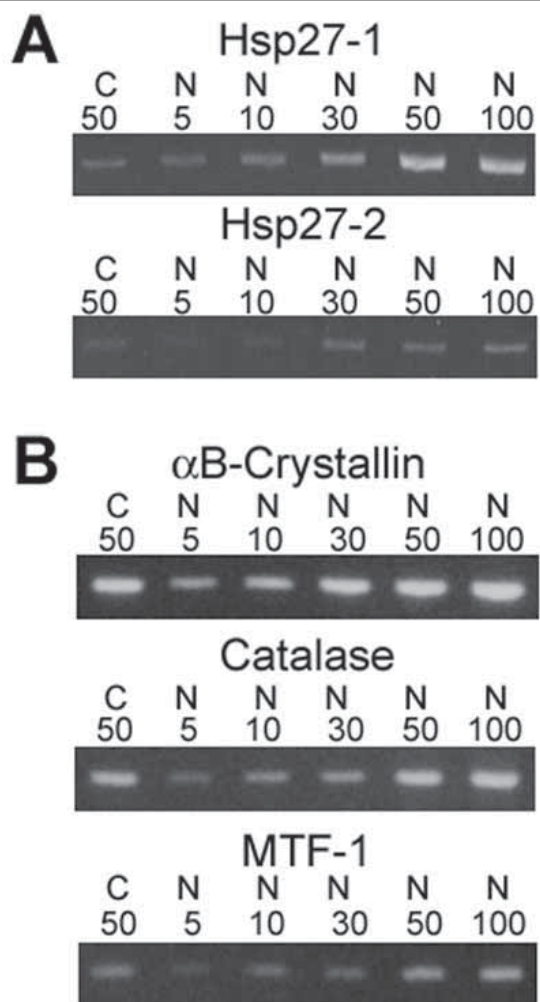


Figure 4. Further RT-PCR confirmation of selected gene expression differences and control genes. RT-PCR confirmation of gene expression differences for HSP27-1 and -2 (**A**) and 3 control genes whose expression levels should be equal between cataract (C) and normal (N) lens epithelia (**B**). The total amount of RNA (ng) used in each reaction is indicated.

TABLE 3. FOLD CHANGES AND DENSITOMETRY VALUES OF RT-PCR CONFIRMATIONS OF THE MICROARRAY DATA

Gene	Fold change in cataracts according to microarray data	Percent adjusted volume for normal lens RNA	Percent adjusted volume for cataractous lens RNA	Calculated densitometry fold change in cataracts
Control genes shown in Figure 4:				
aB-Crystallin	No Change	21.62	17.52	Decreased 1.23 Fold
Catalase	No Change	26.55	18.38	Decreased 1.44 Fold
MTF-1	No Change	22.29	24.46	Increased 1.10 Fold
Primary confirmations shown in Figure 3A:				
Hsp27-1	Decreased 128.00 Fold	72.35	27.65	Decreased 2.62 Fold
aA-Crystallin	Decreased 22.63 Fold	78.27	21.73	Decreased 3.60 Fold
RPL13a	Decreased 2.46 Fold	60.37	39.63	Decreased 1.52 Fold
Metallothionein IF	Decreased 5.66 Fold	74.11	25.89	Decreased 2.86 Fold
Metallothionein IH	Decreased 3.48 Fold	86.92	13.08	Decreased 6.65 Fold
Metallothionein IG	Decreased 3.73 Fold	86.05	13.95	Decreased 6.17 Fold
Glutathione Peroxidase 1	Decreased 4.92 Fold	60.98	39.02	Decreased 1.56 Fold
Na ⁺ /H ⁺ Exchanger II	Increased 6.5 Fold	17.2	82.8	Increased 4.81 Fold
Serine/Threonine Protein Kinase	Increased 6.5 Fold	40.96	59.04	Increased 1.44 Fold
Na ⁺ /K ⁺ ATPase	Increased 8.00 Fold	52.73	47.27	Decreased 1.12 Fold
Secreted Apoptosis Related Protein	Increased 6.06 Fold	17.78	82.22	Increased 4.62 Fold
Pleiotrophin	Increased 7.46 Fold	33.67	66.33	Increased 1.97 Fold
E3-Ubiquitin Ligase	Increased 4.59 Fold	34.84	65.16	Increased 1.87 Fold
Secondary confirmations shown in Figure 3B:				
aA-Crystallin	Decreased 22.63 Fold	57.21	42.79	Decreased 1.34 Fold
RPL13a	Decreased 2.46 Fold	54.29	45.71	Decreased 1.19 Fold
Metallothionein IF	Decreased 5.66 Fold	67.16	32.84	Decreased 2.05 Fold
Na ⁺ /H ⁺ Exchanger II	Increased 6.5 Fold	6.99	93.01	Increased 13.31 Fold
Serine/Threonine Protein Kinase	Increased 6.5 Fold	22.86	77.14	Increased 3.37 Fold
Na ⁺ /K ⁺ ATPase	Increased 8.00 Fold	2.03	97.97	Increased 48.26 Fold
Pleiotrophin	Increased 7.46 Fold	14.78	85.22	Increased 5.77 Fold
Tertiary confirmations shown in Figure 4:				
HSP27-1	Decreased 128 Fold	34.74	4.23	Decreased 8.21 Fold
HSP27-2	Decreased 5.28 Fold	20.49	15.69	Decreased 1.31 Fold

Densitometric analysis of the RT-PCR confirmations shown in Figure 3A,B and Figure 4.

shock protein 27 form 1 was decreased in cataract relative to clear lenses by approximately 10 fold while heat shock protein 27 form 2 was decreased in cataract by approximately 2 fold. Using this same sample of RNA we examined the expression levels of 3 genes (catalase, MTF-1, and α B-crystallin) that were unaltered between cataracts and clear lenses according to the microarray data as a further control. All 3 of these genes exhibited identical expression levels between cataract and normal lens epithelia, as predicted by the microarray analysis (Figure 4).

Densitometric gel scanning of all of the semi-quantitative RT-PCR products described in Figure 3 and Figure 4 was also conducted to further evaluate the data (Table 3). Although all of the calculated fold changes do not exactly match those detected by the microarray hybridization data, they importantly follow the same general trends in gene expression revealed by

the microarray data. These combined confirmations suggest that the gene expression trends revealed by microarray analysis are approximately 84% accurate.

Functional clustering analysis of differentially expressed transcripts: The set of genes that exhibited either increased or decreased expression levels of 2 fold or greater was analyzed for significant enrichment with respect to various categories of gene function using the EASE bioinformatics package. Categories enriched within the mRNAs increased or decreased at the 2 fold or greater level with an EASE score of less than 0.05 are shown in Figure 5, Figure 6, Figure 7, Figure 8, and listed in Table 4. Because many genes have more than one function and are involved in various pathways, many of the identified genes appear in multiple categories.

The entire EASE data set can be accessed in Appendix 1. Statistically significant trends in biological processes (Figure

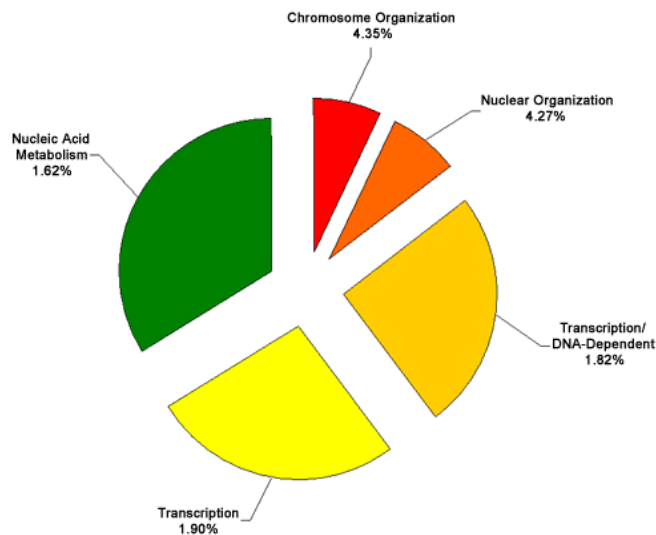


Figure 5. Functional cluster analysis of genes involved in biological processes which have increased expression levels in cataract versus clear lenses. Functional cluster analysis of genes involved in biological processes which have increased expression levels in cataract compared to clear lenses. The specific sub-categories of genes determined to be significantly altered using the statistical clustering program, EASE, are indicated. Percentages indicate the number of altered genes in each sub-category relative to their total representation on the microarray. Colors denote the approximate relative cellular location for which the genes in each sub-category function ranging from the nucleus to the plasma membrane (red to violet). Individual genes in each category are listed in Table 4. Pie piece size approximates the number of changed genes in each sub-category.

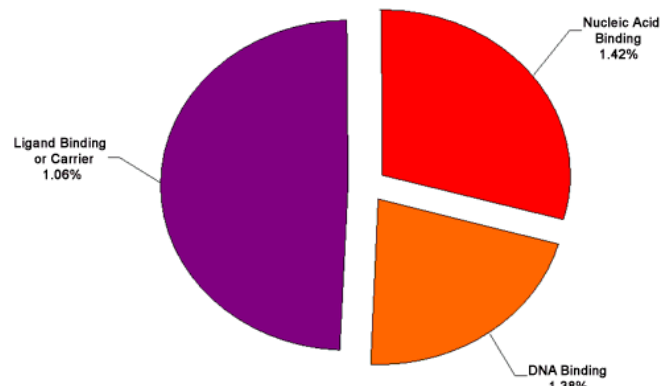


Figure 6. Functional cluster analysis of genes involved in molecular functions which have increased expression levels in cataract versus clear lenses. Functional cluster analysis of genes involved in molecular functions which have increased expression levels in cataract versus clear lenses. The specific sub-categories of genes determined to be significantly altered using the statistical clustering program, EASE, are indicated. Percentages indicate the number of altered genes in each sub-category relative to their total representation on the microarray. Colors denote the approximate relative cellular location for which the genes in each sub-category function ranging from the nucleus to the plasma membrane (red to violet). Individual genes in each category are listed in Table 4. Pie piece size approximates the number of changed genes in each sub-category.

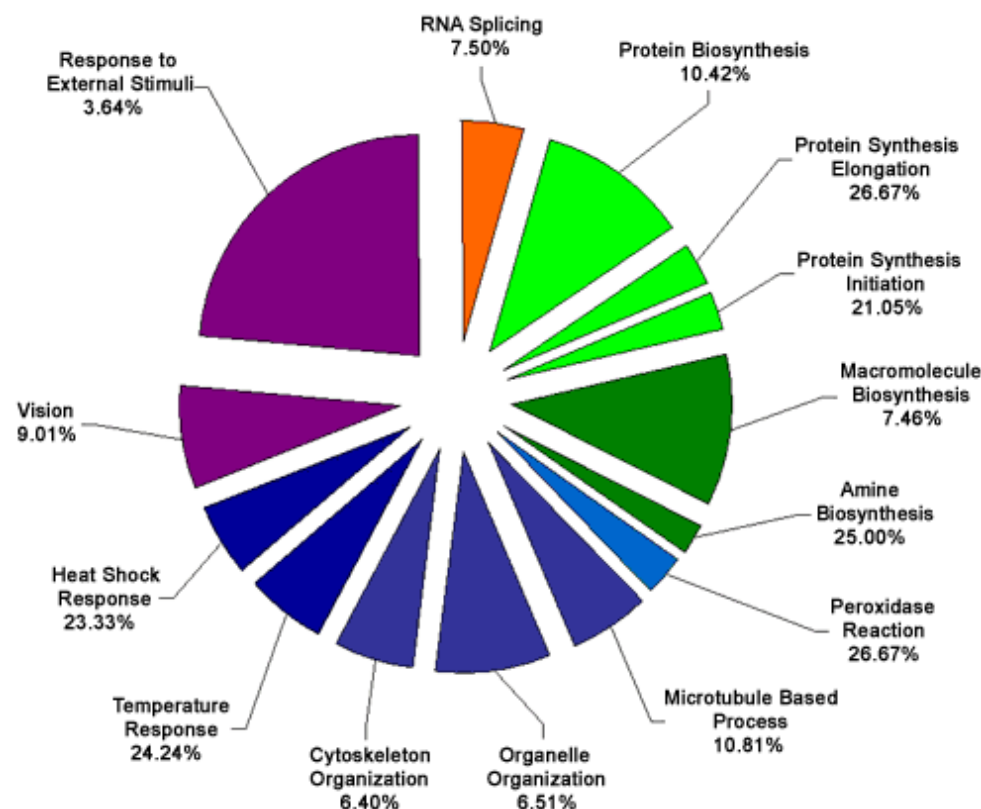


Figure 7. Functional cluster analysis of genes involved in biological processes which have decreased expression levels in cataract versus clear lenses. Functional cluster analysis of genes involved in biological processes which have decreased expression levels in cataract versus clear lenses. The specific sub-categories of genes determined to be significantly altered using the statistical clustering program, EASE, are indicated. Percentages indicate the number of altered genes in each sub-category relative to their total representation on the microarray. Colors denote the approximate relative cellular location for which the genes in each sub-category function ranging from the nucleus to the plasma membrane (red to violet). Individual genes in each category are listed in Table 4. Pie piece size approximates the number of changed genes in each sub-category.

5) and molecular functions (Figure 6) with increased gene expression in cataract were chromosome organization, nuclear organization, transcription/DNA-dependent, transcription, nucleic acid metabolism, nucleic acid binding, ligand binding or carrier, and DNA binding. Statistically significant trends in biological processes (Figure 7) and molecular functions (Figure 8) with decreased gene expression in cataract were RNA splicing, protein biosynthesis, protein synthesis elongation, protein synthesis initiation, macromolecule biosynthesis, amine biosynthesis, peroxidase reaction, microtubule-based process, organelle organization, cytoskeleton organization, temperature response, heat shock response, vision, response to external stimulus, U6 snRNA binding, pre-mRNA splicing factor, mRNA binding, proteasome endopeptidase, translation factor, selenium binding, alcohol dehydrogenase, heat shock protein, oxidoreductase, glutathione peroxidase, chaperone, structural constituents of lens, and structural molecules. Specific examples of the genes included in each category are summarized in Table 4.

DISCUSSION

In the present study, we have compared the relative expression levels of more than half of the genes predicted to comprise the human genome between age-matched cataract and clear human lenses; we have confirmed the accuracy of the data set by semi-quantitative RT-PCR and clustered the differentially expressed genes into functional categories. This analysis has identified over 1,300 genes that are altered in cataract relative to clear lenses. Of these, 74 are increased and 241 are decreased at the 5 fold or greater level between cataract and clear lenses. Although limitations in obtaining sufficient numbers of cataract and clear lenses preclude the extensive

analysis of individual genes at the mRNA and protein level, we estimate that the trends in gene expression detected in the microarray procedure are approximately 84% accurate based on semi-quantitative RT-PCR using separately isolated RNA populations. Although we cannot rule out the possibility that temporal and/or spatial differences between cataract and clear lenses may influence the results of the present study, we are confident that the differences in gene expression detected are truly cataract-specific since the lenses were approximately age-matched (cataract approximately 70.2 years and clear lenses approximately 61.5 years), controlled for the proportion of males and females between the two samples (approximately 45% male), obtained within 24 h post-mortem, and carefully dissected for central epithelium (2-3 mm cataract and 6-8 mm clear). The cataracts examined in this study were mostly mixed and nuclear (70% mixed, 20% nuclear, 5% cortical, and 2% posterior subcapsular) therefore, the effects in gene expression detected in the present survey most likely reflect general gene expression changes associated with age-related cataract and are unlikely to be related to specific types of cataracts, except for possibly nuclear. Large numbers of specific types of cataracts will need to be collected in order to analyze type-specific gene expression patterns. However, it is important to note that many of the same genes and their corresponding magnitude changes detected in the present study correlate almost exactly with the gene expression differences and magnitude changes detected between cataract epithelia and clear lens epithelia using an entirely different population of human subjects as well as a different type of hybridization screening [19,20]. This complementary study provides great confidence in the gene expression differences detected in the present survey.

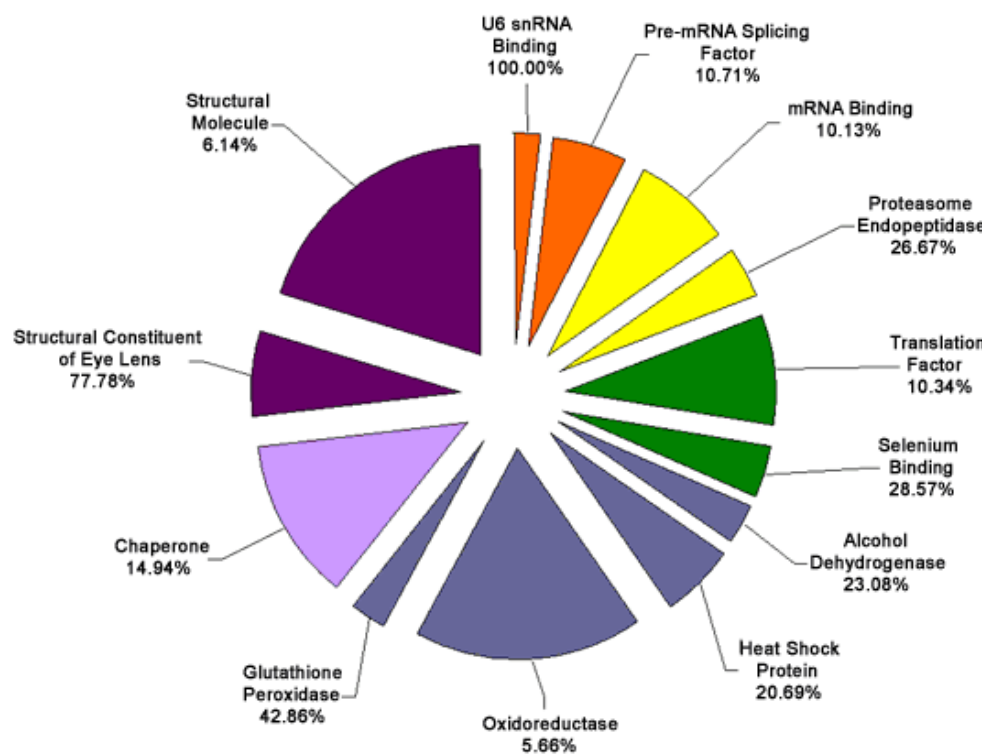


Figure 8. Functional cluster analysis of genes involved in molecular functions which have decreased expression levels in cataract versus clear lenses. Functional cluster analysis of genes involved in molecular functions which have decreased expression levels in cataract versus clear lenses. The specific sub-categories of genes determined to be significantly altered using the statistical clustering program, EASE, are indicated. Percentages indicate the number of altered genes in each sub-category relative to their total representation on the microarray. Colors denote the approximate relative cellular location for which the genes in each sub-category function ranging from the nucleus to the plasma membrane (red to violet). Individual genes in each category are listed in Table 4. Pie piece size approximates the number of changed genes in each sub-category.

TABLE 4. INDIVIDUAL FUNCTIONALLY CLUSTERED GENES

Probe number	Gene name	Accession number	Fold change
Increased In Cataract			
Biological Process			
Chromosome organization			
200679	high-mobility group (nonhistone chromosomal) protein 1	NM_002128	4.5948
205062	retinoblastoma-binding protein 1 (RBBP1)	NM_002892	4.9246
208859	alpha thalassaemia retardation syndrome X-linked	NM_000489	5.6569
209258	chondroitin sulfate proteoglycan 6 (bamacan)	NM_005445	8.5742
209715	heterochromatin protein homologue (HP1)	NM_012117	4.0000
Nuclear organization			
200679	high-mobility group (nonhistone chromosomal) protein 1	NM_000489	4.5948
205062	retinoblastoma-binding protein 1 (RBBP1)	NM_002892	4.9246
208859	alpha thalassaemia retardation syndrome X-linked	NM_000489	5.6569
209258	chondroitin sulfate proteoglycan 6 (bamacan)	NM_005445	8.5742
209715	heterochromatin protein homologue (HP1)	NM_012117	4.0000
Transcription/DNA-dependent			
200679	high-mobility group (nonhistone chromosomal) protein 1	NM_002128	4.5948
201138	Sjogren syndrome antigen B	NM_003142	6.4980
202173	zinc finger protein 161	NM_007146	6.9644
202600	nuclear receptor interacting protein 1	NM_003489	7.4643
202612	cofactor required for Sp1 transcriptional activation, subunit 2	NM_004229	16.0000
204771	transcription termination factor, RNA polymerase I	NM_007344	4.0000
205062	retinoblastoma-binding protein 1 (RBBP1)	NM_002892	4.9246
205070	inhibitor of growth family, member 3	NM_019071	4.2871
205443	small nuclear RNA activating complex	NM_003082	6.9644
205596	E3 ubiquitin ligase Smurf2	NM_022739	4.5948
206848	homeo box A7	NM_006896	4.2871
208003	nuclear factor of activated T-cells 5	NM_006599	4.2871
208859	alpha thalassaemia retardation syndrome X-linked	NM_000489	5.6569
209088	ubiquitin 1	T70262	5.6569
210504	erythroid-specific transcription factor	NM_006563	5.2780
212079	myeloidlymphoid or mixed-lineage leukemia	NM_005933	19.6983
212492	KIAA0876 protein	AW237172	6.9644
Transcription			
200679	high-mobility group (nonhistone chromosomal) protein 1	NM_002128	4.5948
201138	Sjogren syndrome antigen B	NM_003142	6.4980
201606	nuclear phosphoprotein	NM_007062	5.2780
202173	zinc finger protein 161	NM_007146	6.9644
202600	nuclear receptor interacting protein 1	NM_003489	7.4643
202612	cofactor required for Sp1 transcriptional activation, subunit 2	NM_004229	16.0000
204771	transcription termination factor, RNA polymerase I	NM_007344	4.0000
205062	retinoblastoma-binding protein 1 (RBBP1)	NM_002892	4.9246
205070	inhibitor of growth family, member 3	NM_019071	4.2871
205443	small nuclear RNA activating complex	NM_003082	6.9644
205596	E3 ubiquitin ligase Smurf2	NM_022739	4.5948
206848	homeo box A7	NM_006896	4.2871
208003	nuclear factor of activated T-cells 5	NM_006599	4.2871
208859	alpha thalassaemia retardation syndrome X-linked	NM_000489	5.6569
209088	ubiquitin 1	T70262	5.6569
210504	erythroid-specific transcription factor	NM_006563	5.2780
212079	myeloidlymphoid or mixed-lineage leukemia	NM_005933	19.6983
212492	KIAA0876 protein	AW237172	6.9644
Nucleic acid metabolism			

TABLE 4. CONTINUED.

200679	high-mobility group (nonhistone chromosomal) protein 1	NM_002128	4.5948
201138	Sjogren syndrome antigen B	NM_003142	6.4980
201606	nuclear phosphoprotein	NM_007062	5.2780
202173	zinc finger protein 161	NM_007146	6.9644
202600	nuclear receptor interacting protein 1	NM_003489	7.4643
202612	cofactor required for Sp1 transcriptional activation, subunit 2	NM_004229	16.0000
202905	Nijmegen breakage syndrome 1 (nibrin)	NM_002485	6.9644
204771	transcription termination factor, RNA polymerase I	NM_007344	4.0000
205062	retinoblastoma-binding protein 1 (RBBP1)	NM_002892	4.9246
205070	inhibitor of growth family, member 3	NM_019071	4.2871
205443	small nuclear RNA activating complex	NM_003082	6.9644
205596	E3 ubiquitin ligase Smurf2	NM_022739	4.5948
206848	homeo box A7	NM_006896	4.2871
208003	nuclear factor of activated T-cells 5	NM_006599	4.2871
208835	cisplatin resistance-associated overexpressed protein	AW089673	4.2871
208859	alpha thalassaemia retardation syndrome X-linked	NM_000489	5.6569
209024	NS1-associated protein 1	AF037448	4.9246
209088	ubiquitin 1	T70262	5.6569
209579	methyl-CpG binding domain protein 4	NM_003925	4.2871
209715	heterochromatin protein homologue (HP1)	NM_012117	4.0000
210504	erythroid-specific transcription factor	NM_006563	5.2780
212079	myeloidlymphoid or mixed-lineage leukemia	NM_005933	19.6983
212492	KIAA0876 protein	AW237172	6.9644
Molecular Function			
Nucleic acid binding			
200679	high-mobility group (nonhistone chromosomal) protein 1	NM_002128	4.5948
201138	Sjogren syndrome antigen B	NM_003142	6.4980
201635	fragile X mental retardation, autosomal homolog 1	NM_005087	4.5948
202173	zinc finger protein 161	NM_007146	6.9644
202612	cofactor required for Sp1 transcriptional activation, subunit 2	NM_004229	16.0000
202905	Nijmegen breakage syndrome 1 (nibrin)	NM_002485	6.9644
203567	ring finger protein 15	NM_006355	19.6983
204771	transcription termination factor, RNA polymerase I	NM_007344	4.0000
205062	retinoblastoma-binding protein 1 (RBBP1)	NM_002892	4.9246
205070	inhibitor of growth family, member 3	NM_019071	4.2871
206848	homeo box A7	NM_006896	4.2871
208003	nuclear factor of activated T-cells 5	NM_006599	4.2871
208325	lymphoid blast crisis oncogene	NM_006738	4.2871
208624	eukaryotic translation initiation factor 4 gamma	AF104913	6.4980
208859	alpha thalassaemia retardation syndrome X-linked	NM_000489	5.6569
209024	NS1-associated protein 1	AF037448	4.9246
209088	ubiquitin 1	T70262	5.6569
209579	methyl-CpG binding domain protein 4	NM_003925	4.2871
209715	heterochromatin protein homologue (HP1)	NM_012117	4.0000
210504	erythroid-specific transcription factor	NM_006563	5.2780
212079	myeloidlymphoid or mixed-lineage leukemia	NM_005933	19.6983
212492	KIAA0876 protein	AW237172	6.9644
Ligand binding or carrier			
200679	high-mobility group (nonhistone chromosomal) protein 1	NM_002128	4.5948
201138	Sjogren syndrome antigen B	NM_003142	6.4980
201242	ATPase, Na+K+ transporting, beta 1	BC000006	8.0000
201635	fragile X mental retardation, autosomal homolog 1	NM_005087	4.5948
201711	RAN binding protein 2	NM_006267	4.5948
201752	adducin 3 (gamma)	NM_019903	6.0629
201777	KIAA0494 gene product	NM_014774	17.1484
202082	SEC14	NM_003003	4.9246
202118	copine III	NM_003909	6.9644
202173	zinc finger protein 161	NM_007146	6.9644
202600	nuclear receptor interacting protein 1	NM_003489	7.4643
202612	cofactor required for Sp1 transcriptional activation, subunit 2	NM_004229	16.0000

TABLE 4. CONTINUED.

202831	glutathione peroxidase 2	NM_002083	8.0000
202905	Nijmegen breakage syndrome 1 (nibrin)	NM_002485	6.9644
203567	ring finger protein 15	NM_006355	19.6983
204771	transcription termination factor, RNA polymerase I	NM_007344	4.0000
205062	retinoblastoma-binding protein 1 (RBBP1)	NM_002892	4.9246
205070	inhibitor of growth family, member 3	NM_019071	4.2871
205809	Wiskott-Aldrich syndrome-like homeo box A7	NM_003941	14.9285
206848	homeo box A7	NM_006896	4.2871
207152	neurotrophic tyrosine kinase, receptor, type 2	NM_006180	4.0000
208003	nuclear factor of activated T-cells 5	NM_006599	4.2871
208325	lymphoid blast crisis oncogene	NM_006738	4.2871
208624	eukaryotic translation initiation factor 4 gamma	AF104913	6.4980
208859	alpha thalassemialmental retardation syndrome X-linked	NM_000489	5.6569
209024	NS1-associated protein 1	AF037448	4.9246
209088	ubiquitin 1	T70262	5.6569
209258	chondroitin sulfate proteoglycan 6 (bamacan)	NM_005445	8.5742
209466	pleiotrophin	M57399	7.4643
209579	methyl-CpG binding domain protein 4	NM_003925	4.2871
209715	heterochromatin protein homologue (HPL)	NM_012117	4.0000
210504	erythroid-specific transcription factor	NM_006563	5.2780
212079	myeloidlymphoid or mixed-lineage leukemia	NM_005933	19.6983
212492	KIAA0876 protein	AW237172	6.9644
212926	KIAA0594 protein	AW183677	9.1896
214464	Ser-Thr protein kinase	NM_003607	6.4980
214933	calcium channel, voltage-dependent, PQ type, alpha 1A	AA769818	4.9246

DNA binding

200679	high-mobility group (nonhistone chromosomal) protein 1	NM_002128	4.5948
202173	zinc finger protein 161	NM_007146	6.9644
202612	cofactor required for Spl transcriptional activation, subunit 2	NM_004229	16.0000
202905	Nijmegen breakage syndrome 1 (nibrin)	NM_002485	6.9644
204771	transcription termination factor, RNA polymerase I	NM_007344	4.0000
205062	retinoblastoma-binding protein 1 (RBBP1)	NM_002892	4.9246
205070	inhibitor of growth family, member 3	NM_019071	4.2871
206848	homeo box A7	NM_006896	4.2871
208003	nuclear factor of activated T-cells 5	NM_006599	4.2871
208859	alpha thalassemialmental retardation syndrome X-linked	NM_000489	5.6569
209088	ubiquitin 1	T70262	5.6569
209579	methyl-CpG binding domain protein 4	NM_003925	4.2871
209715	heterochromatin protein homologue (HPL)	NM_012117	4.0000
210504	erythroid-specific transcription factor	NM_006563	5.2780
212079	myeloidlymphoid or mixed-lineage leukemia	NM_005933	19.6983
212492	KIAA0876 protein	AW237172	6.9644

Decreased In Cataract

Probe number	Gene name	Accession number	Fold change
Biological Process			
RNA splicing			
200826	small nuclear ribonucleoprotein D2 polypeptide	NM_004597	4.5948
201698	splicing factor, arginineserine-rich 9	NM_003769	6.0629
202567	small nuclear ribonucleoprotein D3 polypeptide	NM_004175	4.5948
204559	U6 snRNA-associated Sm-like protein LSm7	NM_016199	10.5561
208880	putative mitochondrial outer membrane protein import receptor	AB019219	4.5948
209449	SMX5-like protein	AF196468	5.6569
Protein biosynthesis			
200005	eukaryotic translation initiation factor 3, subunit 7	NM_003753	4.9246
200689	eukaryotic translation elongation factor 1 gamma	NM_001404	10.5561

TABLE 4. CONTINUED.

201064	poly(A)-binding protein, cytoplasmic 4	NM_003819	6.9644
201263	threonyl-tRNA synthetase	NM_003191	6.0629
201530	eukaryotic translation initiation factor 4A, isoform 1	NM_001416	4.2871
201632	eukaryotic translation initiation factor 2B, subunit 1	NM_001414	6.0629
201841	heat shock 27 kDa protein 1	NM_001540	128.0000
202021	SUI1 isolog	AF083441	4.5948
202042	histidyl-tRNA synthetase	NM_002109	12.9960
203113	eukaryotic translation elongation factor 1 delta	NM_001960	6.4980
203725	growth arrest and DNA-damage-inducible, alpha	NM_001924	24.2515
204102	eukaryotic translation elongation factor 2	NM_001961	21.1121
208856	ribosomal protein, large, P0	BC003655	4.5948
208887	eukaryotic translation initiation factor 3, subunit 4	BC000733	8.0000
210213	translation initiation factor 6	AF022229	4.0000
Protein synthesis elongation			
200689	eukaryotic translation elongation factor 1 gamma	NM_001404	10.5561
203113	eukaryotic translation elongation factor 1 delta	NM_001960	6.4980
204102	eukaryotic translation elongation factor 2	NM_001961	21.1121
208856	ribosomal protein, large, P0	BC003655	4.5948
Protein synthesis initiation			
201530	eukaryotic translation initiation factor 4A, isoform 1	NM_001416	4.2871
201632	eukaryotic translation initiation factor 2B, subunit 1	NM_001414	6.0629
202021	SUI1 isolog	AF083441	4.5948
210213	translation initiation factor 6	AF022229	4.0000
Macromolecule biosynthesis			
200005	eukaryotic translation initiation factor 3, subunit 7	NM_003753	4.9246
200689	eukaryotic translation elongation factor 1 gamma	NM_001404	10.5561
201064	poly(A)-binding protein, cytoplasmic 4	NM_003819	6.9644
201263	threonyl-tRNA synthetase	NM_003191	6.0629
201530	eukaryotic translation initiation factor 4A, isoform 1	NM_001416	4.2871
201632	eukaryotic translation initiation factor 2B, subunit 1	NM_001414	6.0629
201841	heat shock 27 kDa protein 1	NM_001540	128.0000
202021	SUI1 isolog	AF083441	4.5948
202042	histidyl-tRNA synthetase	NM_002109	12.9960
203113	eukaryotic translation elongation factor 1 delta	NM_001960	6.4980
203725	growth arrest and DNA-damage-inducible, alpha	NM_001924	24.2515
204102	eukaryotic translation elongation factor 2	NM_001961	21.1121
208856	ribosomal protein, large, P0	BC003655	4.5948
208887	eukaryotic translation initiation factor 3, subunit 4	BC000733	8.0000
210213	translation initiation factor 6	AF022229	4.0000
Amine biosynthesis			
200790	ornithine decarboxylase 1	NM_002539	4.9246
201772	antizyme inhibitor	NM_015878	6.9644
207621	phosphatidylethanolamine N-methyltransferase	NM_007169	6.0629
Peroxidase reaction			
200736	glutathione peroxidase 1 (GPX1)	NM_000581	4.9246
201106	glutathione peroxidase 4 (phospholipid hydroperoxidase)	NM_002085	4.2871
201348	glutathione peroxidase 3 (GPX3)	NM_002084	11.3137
212013	KIAA0230 gene	D86983	12.1257
Microtubule-based process			
200712	microtubule-associated protein, RPEB family, member 1	AI633566	10.5561
200750	GTP binding protein	AF054183	4.9246
203690	spindle pole body protein (GCP3)	NM_006322	9.1896
204398	microtubule-associated protein like echinoderm EMAP	NM_012155	4.9246
205191	retinitis pigmentosa 2	NM_006915	12.1257
208786	microtubule-associated proteins 1A1B light chain 3	AF183417	5.6569
208977	tubulin, beta, 2	BC004188	6.0629
209191	Similar to tubulin, beta, 4	BC002654	7.4643
Organelle organization			
200712	microtubule-associated protein, RPEB family, member 1	AI633566	10.5561

TABLE 4. CONTINUED.

200750	GTP binding protein	AF054183	4.9246
200866	saposin proteins A-D	M32221	18.3800
201707	peroxisomal farnesylated protein	NM_002857	4.0000
201821	translocase of inner mitochondrial membrane 17	BC004439	9.1896
203690	spindle pole body protein (GCP3)	NM_006322	9.1896
204398	microtubule-associated protein like echinoderm EMAP	NM_012155	4.9246
205191	retinitis pigmentosa 2	NM_006915	12.1257
208786	microtubule-associated proteins 1A1B light chain 3	AF183417	5.6569
208977	tubulin, beta, 2	BC004188	6.0629
209191	Similar to tubulin, beta, 4	BC002654	7.4643
Cytoskeleton organization			
200712	microtubule-associated protein, RPEB family, member 1	AI633566	10.5561
200750	GTP binding protein	AF054183	4.9246
203690	spindle pole body protein (GCP3)	NM_006322	9.1896
204398	microtubule-associated protein like echinoderm EMAP	NM_012155	4.9246
205191	retinitis pigmentosa 2	NM_006915	12.1257
208786	microtubule-associated proteins 1A1B light chain 3	AF183417	5.6569
208977	tubulin, beta, 2	BC004188	6.0629
209191	Similar to tubulin, beta, 4	BC002654	7.4643
Temperature response			
200064	isolate Liv chaperone protein HSP90 beta	AF275719	4.9246
200664	DnaJ (Hsp40) homolog, subfamily B, member 1	BG537255	6.4980
200797	myeloid cell leukemia sequence 1 (BCL2-related)	AI275690	4.0000
200800	heat shock 70 kDa protein 1A	NM_005345	4.0000
201161	cold shock domain protein A	NM_003651	5.6569
201841	heat shock 27 kDa protein 1	NM_001540	128.0000
202581	heat shock 70 kDa protein 1B	NM_005346	5.6569
205824	heat shock 27 kDa protein 2	NM_001541	5.2780
Heat shock response			
200064	isolate Liv chaperone protein HSP90 beta	AF275719	4.9246
200664	DnaJ (Hsp40) homolog, subfamily B, member 1	BG537255	6.4980
200797	myeloid cell leukemia sequence 1 (BCL2-related)	AI275690	4.0000
200800	heat shock 70 kDa protein 1A	NM_005345	4.0000
201841	heat shock 27 kDa protein 1	NM_001540	128.0000
202581	heat shock 70 kDa protein 1B	NM_005346	5.6569
205824	heat shock 27 kDa protein 2	NM_001541	5.2780
Vision			
201563	L-iditol-2 dehydrogenase	L29008	12.1257
201842	EGF-containing fibulin-like extracellular matrix protein 1	AI826799	4.9246
202766	fibrillin 1	NM_000138	5.2780
204398	microtubule-associated protein like echinoderm EMAP	NM_012155	4.9246
205191	retinitis pigmentosa 2	NM_006915	12.1257
206777	beta B2 crystallin	NM_000496	6.4980
206843	beta A4 crystallin	NM_001886	168.8970
207399	phakinin, beaded filament structural protein 2	NM_003571	12.9960
207532	gamma D crystallin	NM_006891	29.8571
207685	beta B3 crystallin	NM_004076	22.6274
Response to external stimulus			
200064	isolate Liv chaperone protein HSP90 beta	AF275719	4.9246
200664	DnaJ (Hsp40) homolog, subfamily B, member 1	BG537255	6.4980
200797	myeloid cell leukemia sequence 1 (BCL2-related)	AI275690	4.0000
200800	heat shock 70 kDa protein 1A	NM_005345	4.0000
201064	poly(A)-binding protein, cytoplasmic 4	NM_003819	6.9644
201161	cold shock domain protein A	NM_003651	5.6569
201315	interferon induced transmembrane protein 2	NM_006435	4.5948
201348	glutathione peroxidase 3 (GPX3)	NM_002084	11.3137
201563	L-iditol-2 dehydrogenase	L29008	12.1257
201841	heat shock 27 kDa protein 1	NM_001540	128.0000
201842	EGF-containing fibulin-like extracellular matrix protein 1	AI826799	4.9246
201891	beta-2-microglobulin	NM_004048	4.2871
202581	heat shock 70 kDa protein 1B	NM_005346	5.6569
202727	interferon gamma receptor 1	NM_000416	4.0000
202766	fibrillin 1	NM_000138	5.2780
203725	growth arrest and DNA-damage-inducible, alpha	NM_001924	24.2515
203921	carbohydrate (chondroitin 6keratan) sulfotransferase 2	NM_004267	4.5948
204398	microtubule-associated protein like echinoderm EMAP	NM_012155	4.9246

TABLE 4. CONTINUED.

205081	cysteine-rich protein 1	NM_001311	14.9285
205191	retinitis pigmentosa 2	NM_006915	12.1257
205824	heat shock 27 kDa protein 2	NM_001541	5.2780
206777	beta B2 crystallin	NM_000496	6.4980
206843	beta A4 crystallin	NM_001886	168.8970
207399	phakinin, beaded filament structural protein 2	NM_003571	12.9960
207532	gamma D crystallin	NM_006891	29.8571
207685	beta B3 crystallin	NM_004076	22.6274
208650	CD24 antigen	BG327863	4.9246
208791	complement cytolysis inhibitor	M25915	4.2871
208910	pre-mRNA splicing factor 2 p32 subunit	L04636	7.4643
209189	v-fos FBJ murine osteosarcoma viral oncogene homolog	BC004490	12.1257
212013	KIAA0230 gene	D86983	12.1257
216598	monocyte chemotactic protein	S69738	6.4980
Molecular Function			
U6 snRNA binding			
204559	U6 snRNA-associated Sm-like protein LSm7	NM_016199	10.5561
209449	SMX5-like protein	AF196468	5.6569
Pre-mRNA splicing factor			
200826	small nuclear ribonucleoprotein D2 polypeptide	NM_004597	4.5948
201698	splicing factor, arginineserine-rich 9	NM_003769	6.0629
202567	small nuclear ribonucleoprotein D3 polypeptide	NM_004175	4.5948
204559	U6 snRNA-associated Sm-like protein LSm7	NM_016199	10.5561
208880	putative mitochondrial outer membrane protein import receptor	AB019219	4.5948
209449	U6 snRNA-associated Sm-like protein	AF196468	5.6569
mRNA binding			
200826	small nuclear ribonucleoprotein D2 polypeptide	NM_004597	4.5948
201064	poly(A)-binding protein, cytoplasmic 4	NM_003819	6.9644
201530	eukaryotic translation initiation factor 4A, isoform 1	NM_001416	4.2871
201698	splicing factor, arginineserine-rich 9	NM_003769	6.0629
202567	small nuclear ribonucleoprotein D3 polypeptide	NM_004175	4.5948
204559	U6 snRNA-associated Sm-like protein LSm7	NM_016199	10.5561
208880	putative mitochondrial outer membrane protein import receptor	AB019219	4.5948
209449	U6 snRNA-associated Sm-like protein	AF196468	5.6569
Proteasome endopeptidase			
200786	proteasome (prosome,macropain)subunit,beta type, 1	NM_002799	6.0629
200876	proteasome (prosome,macropain)subunit,beta type, 1	NM_002793	8.5742
201532	proteasome (prosome,macropain)subunit,alpa type, 3	NM_002788	5.6569
202243	proteasome (prosome,macropain)subunit,beta type, 4	NM_002796	5.2780
Translation factor			
200005	eukaryotic translation initiation factor 3, subunit 7	NM_003753	4.9246
200689	eukaryotic translation elongation factor 1 gamma	NM_001404	10.5561
201530	eukaryotic translation initiation factor 4A, isoform 1	NM_001416	4.2871
201632	eukaryotic translation initiation factor 2B, subunit 1	NM_001414	6.0629
202021	SUI1 isolog	AF083441	4.5948
203113	eukaryotic translation elongation factor 1 delta	NM_001960	6.4980
204102	eukaryotic translation elongation factor 2	NM_001961	21.1121
208887	eukaryotic translation initiation factor 3, subunit 4	BC000733	8.0000
210213	translation initiation factor 6	AF022229	4.0000
Selenium binding			
200736	glutathione peroxidase 1	NM_000581	4.9246
201106	glutathione peroxidase 4 (phospholipid hydroperoxidase)	NM_002085	4.2871
201194	selenoprotein W, 1 (SEPW1)	NM_003009	6.4980
201348	glutathione peroxidase 3 (GPX3)	NM_002084	11.3137

TABLE 4. CONTINUED.

Alcohol dehydrogenase			
201563	L-Iditol-2 dehydrogenase	L29008	12.1257
210609	quinone oxidoreductase homolog	BC000474	11.3137
213540	beta3-Galactosyltransferase	AL031228	6.0629
Heat shock protein			
200064	isolate Liv chaperone protein HSP90 beta	AF275719	4.9246
200664	DnaJ (Hsp40) homolog, subfamily B, member 1	BG537255	6.4980
200800	heat shock 70 kDa protein 1A	NM_005345	4.0000
201841	heat shock 27 kDa protein 1	NM_001540	128.0000
202581	heat shock 70 kDa protein 1B	NM_005346	5.6569
205824	heat shock 27 kDa protein 2	NM_001541	5.2780
Oxidoreductase			
200736	glutathione peoxidase 1 (GPX1)	NM_000581	4.9246
201106	glutathione peroxidase 4 (phospholipid hydroperoxidase)	NM_002085	4.2871
201194	selenoprotein W, 1 (SEPW1)	NM_003009	6.4980
201348	glutathione peroxidase 3 (GPX3)	NM_002084	11.3137
201563	L-Iditol-2 dehydrogenase	L29008	12.1257
201892	inosine monophosphate dehydrogenase 2 (IMPDH2)	NM_000884	5.2780
202201	biliverdin reductase B(flavin reductase (NADPH))	NM_000713	5.6569
202539	3-hydroxy-3-methylglutaryl-Coenzyme	M11058	
202785	NADH dehydroxygenase (ubiquinone) 1 alpha subcomplex, 7 A reductase	NM_005001	12.9960
202839	NADH dehydroxygenase (ubiquinone) 1 beta subcomplex, 7	NM_004146	4.5948
203570	lysyl oxidase-like 1 (LOXL1)	NM_005576	21.1121
206024	4-hydroxyphenylpyruvate dioxygenase	NM_002150	5.2780
208631	78 kDa gastrin-binding protein	U04627	10.5561
209213	carbonyl reductase 1	BC002511	5.2780
210609	quinone oxidoreductase homolog	BC000474	11.3137
212013	melenoma associated gene	D86983	12.1257
212224	aldehyde dehydrogenase 1 (ALDH1)	AF003341	4.0000
213540	contains BING5 gene, the gene for beta3-galactosyltransferase	AL031228	6.0629
Glutathione peroxidase			
200736	glutathione peroxidase 1 (GPX1)	NM_000581	4.9246
201106	glutathione peroxidase 4 (phospholipid hydroperoxidase)	NM_002085	4.2871
201348	glutathione peroxidase 3 (GPX3)	NM_002084	11.3137
Chaperone			
200064	isolate Liv chaperone protein HSP90 beta	AF275719	4.9246
200664	DnaJ (Hsp40) homolog, subfamily B, member 1	BG537255	6.4980
200800	heat shock 70 kDa protein 1A	NM_005345	4.0000
200812	chaperonin containing TCP1, subunit 7	NM_006429	4.9246
200968	peptidylprolyl isomerase B (cyclophilin B)	NM_000942	17.1484
201459	RuvB	NM_006666	16.0000
201841	heat shock 27 kDa protein 1	NM_001540	128.0000
202416	tetratricopeptide repeat domain 2	NM_003315	6.9644
202581	heat shock 70 kDa protein 1B	NM_005346	5.6569
202843	microvascular endothelial differentiation gene 1	NM_012328	27.8576
205191	retinitis pigmentosa 2	NM_006915	12.1257
205824	heat shock 27 kDa protein 2	NM_001541	5.2780
207132	prefoldin 5	NM_002624	6.9644
Structural constituent of lens			
206746	filensin, beaded filament structural protein 1	NM_001195	17.1484
206777	beta B2 crystallin	NM_000496	6.4980
206778	beta B2 crystallin	NM_000496	12.1257
206843	beta A4 crystallin	NM_001886	168.8970
207399	phakinin, beaded filament structural protein 2	NM_003571	12.9960
207532	gamma D crystallin	NM_006891	29.8571
207685	beta B3 crystallin	NM_004076	22.6274
207715	crystallin, gamma B	NM_005210	6.4980
Structural molecule			
200600	moesin	NM_002444	9.8492
200696	gelsolin	NM_000177	4.2871
201650	keratin 19	NM_002276	4.9246
202007	nidogen (enactin)	BF940043	8.5742
202766	fibrillin 1	NM_000138	5.2780
203690	spindle pole body protein	NM_006322	9.1896
203725	growth arrest and DNA-damage-inducible, alpha	NM_001924	24.2515
205373	catenin (cadherin-associated protein), alpha 2	NM_004389	6.9644
206746	filensin, beaded filament structural protein 1	NM_001195	17.1484

TABLE 4. CONTINUED.

206777	beta B2 crystallin	NM_000496	6.4980
206778	beta B2 crystallin	NM_000496	12.1257
206843	beta A4 crystallin	NM_001886	168.8970
207399	phakinin, beaded filament structural protein 2	NM_003571	12.9960
207532	gamma D crystallin	NM_006891	29.8571
207685	beta B3 crystallin	NM_004076	22.6274
207715	gamma B crystallin	NM_005210	6.4980
208611	alpha II spectrin	U83867	8.0000
208856	ribosomal protein, large, P0	BC003655	4.5948
208977	tubulin, beta, 2	BC004188	6.0629
209191	Similar to tubulin, beta, 4	BC002654	7.4643
210987	tropomyosin	M19267	4.0000
214953	amyloid beta (A4)	X06989	4.0000

The table lists all genes comprising each of the sub-categories that were significantly altered between cataract and clear lenses.

The present study provides evidence for multiple novel differences in gene expression between cataract and clear human lenses. Although descriptions of all of the individual genes that exhibit altered expression are too cumbersome to report, and many of the detected gene expression differences involve ESTs with no known function, some observations can be made. The majority of genes whose expression levels are altered in cataract exhibit decreased expression. These genes function in diverse processes including protein synthesis, oxidative stress, membrane transport, structural proteins, chaperones, and cell cycle control proteins. Many of these processes represent metabolic systems designed to preserve lens homeostasis and their decreased expression may reflect the inability of the lens to maintain its internal environment in the presence of stress and/or cataract. Specific examples of individual genes that exhibit decreased expression in cataract include multiple ribosomal subunits involved in protein synthesis (including large subunits 21, 15, 13a, and 7a which were previously shown to be decreased in cataract relative to clear human lenses) [15], selenoprotein W1, a glutathione dependant antioxidant known to protect lung cells against H₂O₂ cytotoxicity [21] that could play a role in defending the lens against oxidative damage, Na/K ATPase, a membrane transporter likely to be critical for osmotic regulation of the lens (whose proteins levels have previously been shown to be decreased in lens epithelia isolated from human age-related cataract [22]), glutathione peroxidases 1, 3 and 4, important oxidative stress enzymes that are likely to play major roles in lens protection and maintenance [23], ferritin, which has been linked to hereditary hyperferritinemia-cataract syndrome [24], multiple crystallins and other lens structural components, Hsp70, a key ATPase activated chaperone [25], Hsp27-1, a small heat-shock protein likely to be important for lens protection [26], Hsp27-2, a small heat shock protein closely related to αB-crystallin [27] which may also be important for lens protection, and αA-crystallin that, in addition to its structural role in the lens, is also a small heat shock protein that can prevent protein aggregation in the lens [28].

The microarray data showing 21 large and small ribosomal subunit transcripts that have decreased expression levels of 2 fold or greater in cataracts is consistent with differential display results showing that 4 of the large ribosomal subunit transcripts are decreased in cataractous lenses [15]. This process reflects a generalized decrease in protein synthesis in cataractous lens epithelial cells.

We also found significant decreases in genes associated with oxidative stress such as glutathione peroxidase, the metallothionein I genes, quinone oxidoreductase, and transketolase. It has previously been demonstrated that glutathione peroxidase-1-deficient mice develop cataracts at an early age [23] and that the levels of glutathione peroxidase are significantly decreased in the plasma of patients with senile cataracts [29]. It is also known that oxidative stress occurs when the quinone oxidoreductase gene is damaged resulting in the production of oxygen radicals [30]. The down regulation of the quinone oxidoreductase gene would also result in the same outcome, an increase in the overall production of oxygen radicals. Others have shown that the loss of transketolase function, an enzyme that catalyzes two of three reactions for entry into the pentose-phosphate pathway, a major source of chemical reducing power, results in lens fiber cell degeneration [31].

Another major functional category exhibiting decreased gene expression in cataracts is the small heat shock proteins/chaperones. Small heat shock proteins (sHSPs) are a large family of proteins that, unlike the large HSPs that are mainly involved in protein folding, play an important role in protecting organisms against stress [26]. This study specifically found rather large decreases in many of the crystallin proteins as well as HSP27. Mice lacking the α A-crystallin gene develop cataracts at an early age [32] and a missense mutation in the gene has been genetically linked to one form of autosomal dominant congenital cataracts in mice [33] and humans [34,35].

Many of the genes encoding structural lens proteins also exhibited decreased expression in cataract. This includes many of the β - and γ -crystallins which are thought to be essential for lens clarity and refraction. Indeed, mutations in β -crystallin has also been related to cataract formation, including a nonsense mutation in β B1-crystallin [36] and a mutation in the β B2-crystallin gene [37]. Two other genes involved in lens structure are filensin and phakinin. These two genes together make up the lens-specific intermediate filament known as the Beaded Filament [38]. It has been shown that the filensin protein is absent in lenses that have posterior subcapsular cataracts [39].

One additional functional category exhibiting decreased expression in cataractous lenses is the cyclins. This includes cyclin D1, cyclin G1, and BCL-1. Although there are very few reports examining the roles of these genes in the lens or their effects, if any, on cataract formation, one group of researchers has demonstrated that overexpression of cyclin G1 in fetal human lens epithelial cells results in an increased incidence of apoptosis [40].

Fewer genes exhibited increased expression in cataract. These genes function in processes as diverse as transcriptional control, ion transport, cytoplasmic transport, ion regulation, Ca^{2+} homeostasis, protein salvaging pathways, and extracellular matrix interactions. Many of the pathways that exhibit increased expression in cataract are also associated with transcriptional processes that may represent attempts by the lens to compensate for stresses related to cataract. Specific examples of individual genes include multiple zinc finger pro-

teins (important for transcriptional regulation), Na/H exchangers (which play key roles in regulating intracellular pH levels [41]), multiple calcium transporters and chloride channels (important for the maintenance of cellular homeostasis), osteonectin (a calcium-binding protein that functions in the regulation of cell growth [42]), and adducin (a member of a gene family encoding cytoskeletal proteins [43]).

According to the EASE analysis, functionally related groups of genes that exhibit overall trends of increased expression in cataracts include peptidyl-prolyl *cis-trans* isomerases. Twenty five percent of cyclophilin-like peptidyl-prolyl *cis-trans* isomerases present on the microarray exhibited increased gene expression in cataract including RAN binding protein. The peptidyl-prolyl *cis-trans* isomerases catalyze the *cis-trans* isomerization of prolyl-peptide bonds [44-46]. Some peptidyl-prolyl *cis-trans* isomerases may also possess chaperone activity by binding to and inhibiting the formation of misfolded protein aggregates [47-49]. It is possible that these isomerases are increased in cataracts in an attempt to prevent the aggregation of proteins in the lens which occur during cataract formation. Splice variants of a new class of cyclophilin-related proteins, types I and II, have been isolated [50,51] and it was found that the type II isoform is identical to Ran-binding protein 2 (RanBP2) [52,53].

Ran-binding protein 2 is a component of the nuclear pore complex which mediates macromolecular transport between the nucleus and the cytoplasm of the cell and serves the cell's requirement for bi-directional, selective, diverse and high-volume transport between these two compartments [54]. Thirty to 40 different proteins, called nucleoporins, have been identified as components of the nuclear pore complex [55]. RanBP2, which exhibited increased expression in cataracts, is the largest nucleoporin and has been localized to the cytoplasmic filaments of the nuclear pore complex [56]. RanBP1, another cytosolic protein closely related to RanBP2, is also involved in nuclear transport [57] and exhibits increased expression in cataracts.

In addition to cytoplasmic transport, many genes associated with ionic transport also exhibit increased expression in cataracts. One gene in particular, cullin 5, which shares 96% homology with vasopressin-activated Ca^{2+} -mobilizing receptor, is increased in cataract. Although its specific function is currently unknown, it is likely to be involved in the Ca^{2+} and cAMP dependent cell signaling pathways [58]. Organ culture studies of the bovine lens demonstrate that a marked decrease in protein synthesis and a net leakage of proteins is strongly associated with an increase in calcium concentration [59]. The activity of Ca^{2+} -ATPase has also been shown to be reduced by 50% in the membranes of lens epithelia isolated from cataractous lenses compared to clear human lenses [60]. Oxidative stress has also been demonstrated to have an effect on the activity of Ca^{2+} transporters in the lens. For example, hydrogen peroxide decreases the activity of Ca^{2+} transporters in rabbit lenses [61]. These phenomenon are closely associated with our results demonstrating an increase in Ca^{2+} transporters, possibly in an attempt to overcome their decreased activity in cataractous lenses, as well as a decrease in genes associated

with protein synthesis.

Another ion channel that demonstrated increased expression in cataracts is the Na⁺/H⁺ exchanger isoform 2. Electroneutral Na⁺-H⁺ exchange is present in virtually all cell types and mediates the exchange of extracellular Na⁺ for intracellular H⁺ and therefore plays an important role in regulating the intracellular pH level, cell volume, and transepithelial Na⁺ absorption [41]. Intracellular pH can affect many cell functions such as metabolic activity, protein synthesis, and cell growth rates [62]. Previous studies have demonstrated that the Na⁺/H⁺ exchangers play a significant role in regulating the intracellular pH of cultured bovine lens epithelial cells [63]. It is also known that the type I Na⁺/H⁺ exchanger is activated by hypertonicity in many cell types [64] and the epithelial cells of toad lenses exposed to hypertonic conditions become acidified, stimulating the Na⁺/H⁺ exchanger to return the pH of the epithelial cells back to normal levels [65].

Another major group of genes that exhibit increased expression in cataractous epithelia compared to normal clear epithelia encode extracellular matrix proteins. Specifically, adducin, a family member of genes encoding cytoskeletal proteins [43], was increased in cataract. A second gene, pleiotrophin, which is also an extracellular matrix protein that binds heparin [66] and is induced during wound repair [67], was also increased in cataracts. Claudin, a component of tight junction filaments capable of interacting adhesively with complementary molecules on adjacent epithelial cells [68], also exhibited increased expression in cataracts. Recent studies have found that overexpression of claudin-2 induces cation-selective channels in tight junctions of epithelial cells resulting in increased ion permeability [69]. Another extracellular matrix gene whose expression is increased in cataracts is supervillin, an F-actin bundling plasma membrane protein that contains functional nuclear localization signals [70]. Bamacan, a chondroitin sulfate proteoglycan that abounds in basement membranes and is thought to be involved in the control of cell growth and transformation [71], also exhibited increased expression in cataracts. One final extracellular matrix gene that was increased in cataracts is Osteonectin which has previously been demonstrated to be increased in human age-related cataracts [72].

In summary this report identifies the global gene expression changes associated with age-related cataract and provides evidence for specific biological pathways that are associated with this disease. It is not possible from this study to determine whether these gene expression differences are a cause of cataract formation or a response of the lens to the presence of the cataract. However, future confirmation at the protein level and functional analysis of the identified genes in tissue culture and animal model systems will eventually help define the individual roles that the identified genes play in lens maintenance, protection, and cataract. Analysis of the identified pathways will yield important information concerning the regulation of gene expression in age-related cataract and may aid in the development of therapeutic treatments to prevent or delay the onset of this disease.

ACKNOWLEDGEMENTS

The authors thank Divyen Patel of Genome Explorations Inc., for his technical advice and services, Tracy Cowell and Erik Peterson of the Kantorow laboratory for their suggestions and help throughout the course of this project and the Lions Eye Bank of Oregon and the West Virginia Eye Bank for providing the clear lenses used in this study. This research was supported by NIH grants EY13022 (MK) and EY03897 (JH).

REFERENCES

1. Bron A, Brown NP. Biology of cataract. In: *Lens Disorders: A Clinical Manual of Cataract Diagnosis*. Oxford, UK: Butterworth-Heinemann; 1996. p. 53-77.
2. Piatigorsky J. Lens differentiation in vertebrates. A review of cellular and molecular features. *Differentiation* 1981; 19:134-53.
3. Bloemendal H. Lens Proteins. In: Bloemendal H, editor. *Molecular and cellular biology of the eye lens*. New York: Wiley; 1981. p. 1-47.
4. Reddy VN. Metabolism of glutathione in the lens. *Exp Eye Res* 1971; 11:310-28.
5. Spector A. Aging of the lens and cataract formation. In: Sekuler R, Kline D, Dismukes K, editors. *Aging and human visual function*. New York: A.R. Liss; 1982. p. 27-43.
6. Reddan JR. Control of cell division in the ocular lens, retina and vitreous humour. In: *Cell biology of the eye*. McDevitt DS, editor. New York: Academic Press; 1982. p. 299-375.
7. Rae JL, Bartling C, Rae J, Mathias RT. Dye transfer between cells of the lens. *J Membr Biol* 1996; 150:89-103.
8. Harding JJ, Crabbe MJC. The lens: development, proteins, metabolism and cataract. In: Davson H, editor. *The eye*. Vol 1B. Orlando (FL): Academic Press; 1984. p. 207-492.
9. Spector A. Oxidative stress-induced cataract: mechanism of action. *FASEB J* 1995; 9:1173-82.
10. Hightower KR. The role of the lens epithelium in development of UV cataract. *Curr Eye Res* 1995; 14:71-8.
11. Kantorow M, Kays T, Horwitz J, Huang Q, Sun J, Piatigorsky J, Carper D. Differential display detects altered gene expression between cataractous and normal human lenses. *Invest Ophthalmol Vis Sci* 1998; 39:2344-54.
12. Kantorow M, Horwitz J, Carper D. Up-regulation of osteonectin/SPARC in age-related cataractous human lens epithelia. *Mol Vis* 1998; 4:17.
13. Wan XH, Lee EH, Koh HJ, Song J, Kim EK, Kim CY, Lee JB, Kim SY, Yao K, Lee JH. Enhanced expression of transglutaminase 2 in anterior polar cataracts and its induction by TGF-beta in vitro. *Br J Ophthalmol* 2002; 86:1293-8.
14. Lee EH, Seomun Y, Hwang KH, Kim JE, Kim IS, Kim JH, Joo CK. Overexpression of the transforming growth factor-beta-inducible gene betaig-h3 in anterior polar cataracts. *Invest Ophthalmol Vis Sci* 2000; 41:1840-5.
15. Zhang W, Hawse J, Huang Q, Sheets N, Miller KM, Horwitz J, Kantorow M. Decreased expression of ribosomal proteins in human age-related cataract. *Invest Ophthalmol Vis Sci* 2002; 43:198-204.
16. Lim JM, Lee JH, Wee WR, Joo CK. Downregulated expression of ADAM9 in anterior polar cataracts. *J Cataract Refract Surg* 2002; 28:697-702.
17. Goswami S, Sheets NL, Zavadil J, Chauhan BK, Bottinger EP, Reddy VN, Kantorow M, Cvekl A. Spectrum and range of oxidative stress responses of human lens epithelial cells to H₂O₂ insult. *Invest Ophthalmol Vis Sci* 2003; 44:2084-93.
18. Spector A, Li D, Ma W, Sun F, Pavlidis P. Differential amplifica-

- tion of gene expression in lens cell lines conditioned to survive peroxide stress. *Invest Ophthalmol Vis Sci* 2002; 43:3251-64.
19. Maraini G, Ruotolo R, Rivetti C, Percudani R, Ottonello S. DNA array analysis of gene expression in the lens epithelium of pure nuclear cataract and transparent human lenses. ARVO Annual Meeting; 2002 May 5-10; Fort Lauderdale, FL.
 20. Ruotolo R, Grassi F, Percudani R, Rivetti C, Martorana D, Maraini G, Ottonello S. Gene expression profiling in human age-related nuclear cataract. *Mol Vis* 2003; 9: 538-48.
 21. Jeong D, Kim TS, Chung YW, Lee BJ, Kim IY. Selenoprotein W is a glutathione-dependent antioxidant in vivo. *FEBS Lett* 2002; 517:225-8.
 22. Tseng SH, Tang MJ. Na,K-ATPase in lens epithelia from patients with senile cataracts. *J Formos Med Assoc* 1999; 98:627-32.
 23. Reddy VN, Giblin FJ, Lin LR, Dang L, Unakar NJ, Musch DC, Boyle DL, Takemoto LJ, Ho YS, Knoernschild T, Juenemann A, Lutjen-Drecoll E. Glutathione peroxidase-1 deficiency leads to increased nuclear light scattering, membrane damage, and cataract formation in gene-knockout mice. *Invest Ophthalmol Vis Sci* 2001; 42:3247-55.
 24. Martin ME, Fargion S, Brissot P, Pellat B, Beaumont C. A point mutation in the bulge of the iron-responsive element of the L ferritin gene in two families with the hereditary hyperferritinemia-cataract syndrome. *Blood* 1998; 91:319-23.
 25. Haslbeck M. sHsps and their role in the chaperone network. *Cell Mol Life Sci* 2002; 59:1649-57.
 26. Ganea E. Chaperone-like activity of alpha-crystallin and other small heat shock proteins. *Curr Protein Pept Sci* 2001; 2:205-25.
 27. Iwaki A, Nagano T, Nakagawa M, Iwaki T, Fukumaki Y. Identification and characterization of the gene encoding a new member of the alpha-crystallin/small hsp family, closely linked to the alphaB-crystallin gene in a head-to-head manner. *Genomics* 1997; 45:386-94.
 28. Horwitz J. Alpha-crystallin can function as a molecular chaperone. *Proc Natl Acad Sci U S A* 1992; 89:10449-53.
 29. Xue AN, Cai QY, Wang SQ, Zhou AS, Li WX, Fu P, Chen XS. Antioxidant status in persons with and without senile lens changes. *Biomed Environ Sci* 1996; 9:144-8.
 30. Pitkanen S, Robinson BH. Mitochondrial complex I deficiency leads to increased production of superoxide radicals and induction of superoxide dismutase. *J Clin Invest* 1996; 98:345-51.
 31. Frederikse PH, Farnsworth P, Zigler JS Jr. Thiamine deficiency in vivo produces fiber cell degeneration in mouse lenses. *Biochem Biophys Res Commun* 1999; 258:703-7.
 32. Brady JP, Garland D, Duglas-Tabor Y, Robison WG Jr, Groome A, Wawrousek EF. Targeted disruption of the mouse alpha A-crystallin gene induces cataract and cytoplasmic inclusion bodies containing the small heat shock protein alpha B-crystallin. *Proc Natl Acad Sci U S A* 1997; 94:884-9.
 33. Cobb BA, Petrash JM. Structural and functional changes in the alpha A-crystallin R116C mutant in hereditary cataracts. *Biochemistry* 2000; 39:15791-8.
 34. Litt M, Kramer P, LaMorticella DM, Murphey W, Lovrien EW, Weleber RG. Autosomal dominant congenital cataract associated with a missense mutation in the human alpha crystallin gene CRYAA. *Hum Mol Genet* 1998; 7:471-4.
 35. Pras E, Frydman M, Levy-Nissenbaum E, Bakhan T, Raz J, Assia EI, Goldman B, Pras E. A nonsense mutation (W9X) in CRYAA causes autosomal recessive cataract in an inbred Jewish Persian family. *Invest Ophthalmol Vis Sci* 2000; 41:3511-5.
 36. Mackay DS, Boskovska OB, Knopf HL, Lampi KJ, Shiels A. A nonsense mutation in CRYBB1 associated with autosomal dominant cataract linked to human chromosome 22q. *Am J Hum Genet* 2002; 71:1216-21.
 37. Graw J, Loster J, Soewarto D, Fuchs H, Reis A, Wolf E, Balling R, de Angelis MH. Aey2, a new mutation in the betaB2-crystallin-encoding gene of the mouse. *Invest Ophthalmol Vis Sci* 2001; 42:1574-80.
 38. Gounari F, Karagianni N, Mincheva A, Lichter P, Georgatos SD, Schirmacher V. The mouse filensin gene: structure and evolutionary relation to other intermediate filament genes. *FEBS Lett* 1997; 413:371-8.
 39. Hess JF, Casselman JT, Kong AP, FitzGerald PG. Primary sequence, secondary structure, gene structure, and assembly properties suggests that the lens-specific cytoskeletal protein filensin represents a novel class of intermediate filament protein. *Exp Eye Res* 1998; 66:625-44.
 40. Kampmeier J, Behrens A, Wang Y, Yee A, Anderson WF, Hall FL, Gordon EM, McDonnell PJ. Inhibition of rabbit keratocyte and human fetal lens epithelial cell proliferation by retrovirus-mediated transfer of antisense cyclin G1 and antisense MAT1 constructs. *Hum Gene Ther* 2000; 11:1-8.
 41. Sangan P, Rajendran VM, Geibel JP, Binder HJ. Cloning and expression of a chloride-dependent Na⁺-H⁺ exchanger. *J Biol Chem* 2002; 277:9668-75.
 42. Sage EH, Bassuk JA, Yost JC, Folkman MJ, Lane TF. Inhibition of endothelial cell proliferation by SPARC is mediated through a Ca(2+)-binding EF-hand sequence. *J Cell Biochem* 1995; 57:127-40.
 43. Gilligan DM, Sarid R, Weese J. Adducin in platelets: activation-induced phosphorylation by PKC and proteolysis by calpain. *Blood* 2002; 99:2418-26.
 44. Schmid FX. Prolyl isomerase: enzymatic catalysis of slow protein-folding reactions. *Annu Rev Biophys Biomol Struct* 1993; 22:123-42.
 45. Rudd KE, Sofia HJ, Koonin EV, Plunkett G 3rd, Lazar S, Rouviere PE. A new family of peptidyl-prolyl isomerases. *Trends Biochem Sci* 1995; 20:12-4.
 46. Rassow J, Pfanner N. Protein biogenesis: chaperones for nascent polypeptides. *Curr Biol* 1996; 6:115-8.
 47. Freskgard PO, Bergenhem N, Jonsson BH, Svensson M, Carlsson U. Isomerase and chaperone activity of prolyl isomerase in the folding of carbonic anhydrase. *Science* 1992; 258:466-8.
 48. Lilie H, Lang K, Rudolph R, Buchner J. Prolyl isomerases catalyze antibody folding in vitro. *Protein Sci* 1993; 2:1490-6.
 49. Rinfret A, Collins C, Menard R, Anderson SK. The N-terminal cyclophilin-homologous domain of a 150-kilodalton tumor recognition molecule exhibits both peptidylprolyl cis-trans-isomerase and chaperone activities. *Biochemistry* 1994; 33:1668-73.
 50. Ferreira PA, Pak WL. Characterization of vertebrate homologs of Drosophila photoreceptor proteins In: Anderson RE, LaVail MM, Holyfield JG, editors. Degenerative diseases of the retina. New York: Plenum Press; 1995. p. 263-274.
 51. Ferreira PA, Hom JT, Pak WL. Retina-specifically expressed novel subtypes of bovine cyclophilin. *J Biol Chem* 1995; 270:23179-88.
 52. Yokoyama N, Hayashi N, Seki T, Pante N, Ohba T, Nishii K, Kuma K, Hayashida T, Miyata T, Aebi U, Fukui M, Nishimoto T. A giant nucleopore protein that binds Ran/TC4. *Nature* 1995; 376:184-8.
 53. Wu J, Matunis MJ, Kraemer D, Blobel G, Coutavas E. Nup358, a cytoplasmically exposed nucleoporin with peptide repeats, Ran-GTP binding sites, zinc fingers, a cyclophilin A homologous domain, and a leucine-rich region. *J Biol Chem* 1995;

- 270:14209-13.
54. Walther TC, Pickersgill HS, Cordes VC, Goldberg MW, Allen TD, Mattaj JW, Fornerod M. The cytoplasmic filaments of the nuclear pore complex are dispensable for selective nuclear protein import. *J Cell Biol* 2002; 158:63-77.
 55. Rout MP, Aitchison JD. Pore relations: nuclear pore complexes and nucleocytoplasmic exchange. *Essays Biochem* 2000; 36:75-88.
 56. Wilken N, Senecal JL, Scheer U, Dabauvalle MC. Localization of the Ran-GTP binding protein RanBP2 at the cytoplasmic side of the nuclear pore complex. *Eur J Cell Biol* 1995; 68:211-9.
 57. Gorlich D, Kutay U. Transport between the cell nucleus and the cytoplasm. *Annu Rev Cell Dev Biol* 1999; 15:607-60.
 58. Burnatowska-Hledin M, Zhao P, Capps B, Poel A, Parmelee K, Mungall C, Sharangpani A, Listenberger L. VACM-1, a cullin gene family member, regulates cellular signaling. *Am J Physiol Cell Physiol* 2000; 279:C266-73.
 59. Duncan G, Jacob TJ. Calcium and the physiology of cataract. *Ciba Found Symp* 1984; 106:132-52.
 60. Paterson CA, Zeng J, Hussein Z, Borchman D, Delamere NA, Garland D, Jimenez-Asensio J. Calcium ATPase activity and membrane structure in clear and cataractous human lenses. *Curr Eye Res* 1997; 16:333-8.
 61. Borchman D, Paterson CA, Delamere NA. Oxidative inhibition of Ca²⁺-ATPase in the rabbit lens. *Invest Ophthalmol Vis Sci* 1989; 30:1633-7.
 62. Bonanno JA. Regulation of corneal epithelial intracellular pH. *Optom Vis Sci* 1991; 68:682-6.
 63. Williams MR, Duncan G, Croghan PC, Riach R, Webb SF. pH regulation in tissue-cultured bovine lens epithelial cells. *J Membr Biol* 1992; 129:179-87.
 64. Garnovskaya MN, Mukhin YV, Vlasova TM, Raymond JR. Hypertonicity activates Na⁺/H⁺ exchange through Janus kinase 2 and calmodulin. *J Biol Chem* 2003; 278:16908-15.
 65. Wolosin JM, Alvarez LJ, Candia OA. Stimulation of toad lens epithelial Na⁺/H⁺ exchange activity by hypertonicity. *Exp Eye Res* 1989; 48:855-62.
 66. Fath M, VanderNoot V, Kilpelainen I, Kinnunen T, Rauvala H, Linhardt RJ. Interaction of soluble and surface-bound heparin binding growth-associated molecule with heparin. *FEBS Lett* 1999; 454:105-8.
 67. Deuel TF, Zhang N, Yeh HJ, Silos-Santiago I, Wang ZY. Pleiotrophin: a cytokine with diverse functions and a novel signaling pathway. *Arch Biochem Biophys* 2002; 397:162-71.
 68. Gonzalez-Mariscal L, Betanzos A, Nava P, Jaramillo BE. Tight junction proteins. *Prog Biophys Mol Biol* 2003; 81:1-44.
 69. Amasheh S, Meiri N, Gitter AH, Schoneberg T, Mankertz J, Schulzke JD, Fromm M. Claudin-2 expression induces cation-selective channels in tight junctions of epithelial cells. *J Cell Sci* 2002; 115:4969-76.
 70. Wulfschlegel JD, Donina IE, Stark NH, Pope RK, Pestonjama KN, Niswonger ML, Luna EJ. Domain analysis of supervillin, an F-actin bundling plasma membrane protein with functional nuclear localization signals. *J Cell Sci* 1999; 112 (Pt 13):2125-

Appendix 1. Raw affymetrix chip data with EASE analysis

These files are the raw affymetrix data and the entire EASE data analysis. The file entitled "raw-data.txt" is a list of all of the genes that are either increased or decreased by 2 fold or greater levels according to the affymetrix chip data. The list includes each gene's relative signal intensity, statistical probability, and description. The file entitled "increased-2-fold.txt" represents the EASE analysis data for all of the genes that are increased by 2 fold or greater levels according to the microarray data with the statistical analysis for each of the categories. This is the data that was used to create Figure 5 and Figure 6. The file entitled "decreased-2-fold.txt" represents the EASE analysis data for all of the genes that are decreased by 2 fold or greater levels according to the microarray data with the statistical analysis for each of the categories. This is the data that was used to create Figure 7 and Figure 8. The file entitled "scatter-plot.jpg" is a graphical representation of the expression differences between cataract and clear lenses. The Y-axis is the signal intensity value of the clear lens hybridization versus the cataract hybridization. The X-axis is the cataract signal intensity value. Each dot on this graph represents an individual gene. The blue dots are genes increased in cataract while the red dots represent genes decreased in cataract. The green lines indicate fold-change values with the two most exterior lines representing 10 fold and the two most interior lines represent 2 fold changes. The middle lines represent 3 fold changes.

To access this data, click or select the words "data and analysis" in the online version of this article. This will initiate the download of a compressed (zip) archive. This file should be uncompressed with an appropriate program (the particular program will depend on your operating system). Once extracted, you will have a folder (or directory) containing eight files (one for each microarray). The files are tab delimited text. Most spreadsheet programs will import files in this format.